

# Biconvex Clustering

Saptarshi Chakraborty<sup>1</sup> and Jason Xu<sup>\*2</sup>

<sup>1</sup>Department of Statistics, University of California, Berkeley

<sup>2</sup>Department of Statistical Science, Duke University

## Abstract

Convex clustering has recently garnered increasing interest due to its attractive theoretical and computational properties. While it confers many advantages over traditional clustering methods, its merits become limited in the face of high-dimensional data. In such settings, not only do Euclidean measures of fit appearing in the objective provide weaker discriminating power, but pairwise affinity terms that rely on  $k$ -nearest neighbors become poorly specified. We find that recent attempts which successfully address the former difficulty still suffer from the latter, in addition to incurring high computational cost and some numerical instability. To surmount these issues, we propose to modify the convex clustering objective so that feature weights are optimized jointly with the centroids. The resulting problem becomes biconvex and as such remains well-behaved statistically and algorithmically. In particular, we derive a fast algorithm with closed form updates and convergence guarantees, and establish finite-sample bounds on its prediction error that imply consistency. Our biconvex clustering method performs feature selection throughout the clustering task: as the learned weights change the effective feature representation, pairwise affinities can be updated adaptively across iterations rather than precomputed within a dubious feature space. We validate the contributions on real and simulated data, showing that our method effectively addresses the challenges of dimensionality while reducing dependence on carefully tuned heuristics typical of existing approaches.

*Keywords:* Sparse clustering, Variable Weighing, Convex Optimization, Feature Selection, Finite sample error bounds.

## 1 Introduction and background

Clustering is a cornerstone of unsupervised learning that seeks to partition unlabeled data into groups according to some measure of similarity. Classical approaches such as  $k$ -means clustering (MacQueen et al., 1967) typically formulate the task as a non-convex optimization problem and seek a solution via a greedy algorithm. Such methods are often effective in practice and have endured due to their simplicity, but also

---

\*Correspondence to: jason.q.xu@duke.edu

suffer from well-documented shortcomings (Jain, 2010). These include requiring prior knowledge or tuning of the number of clusters  $k$  as input (Tibshirani et al., 2001; Hamerly and Elkan, 2004), as well as instability and sensitivity to initial conditions due to non-convexity (Ostrovsky et al., 2013; Xu and Lange, 2019), and deteriorating performance in high dimensions (Witten and Tibshirani, 2010; de Amorim, 2016; Chakraborty and Das, 2019).

While ongoing research continues to combat the shortcomings of algorithms such as  $k$ -means through effective seeding schemes and annealing techniques (Bachem et al., 2016; Xu and Lange, 2019), an alternative approach is to study convex relaxations of traditionally non-convex problems (Tropp, 2006). Convex clustering, also called sum-of-norms clustering, has recently garnered growing interest due to its attractive theoretical properties and viable algorithms (Pelckmans et al., 2005; Hocking et al., 2011; Lindsten et al., 2011). Given data  $\mathbf{X} \in \mathbb{R}^{n \times p}$  and denoting the  $j$ th row of a matrix  $\mathbf{Z}$  as  $\mathbf{z}_{j\cdot}$ , the convex clustering objective is given by

$$\min_{\boldsymbol{\mu}} \frac{1}{2} \sum_{i=1}^n \|\mathbf{x}_i - \boldsymbol{\mu}_i\|_2^2 + \gamma \sum_{i < j} \phi_{ij} \|\boldsymbol{\mu}_i - \boldsymbol{\mu}_j\|_q. \quad (1)$$

Here  $\|\cdot\|_q$  denote the  $\ell_q$  norm,  $q \in \mathbb{N}$ . Each row of the optimization variable  $\boldsymbol{\mu} \in \mathbb{R}^{n \times p}$  represents a cluster center. The first term of (1) is a measure of fit between the data points  $\mathbf{X}$  and the solution  $\boldsymbol{\mu}$ ; the latter is a fusion term that penalizes the number of unique centers or rows of  $\boldsymbol{\mu}$  by way of an  $\ell_q$  norm penalty with tuning constant  $\gamma > 0$ . The approach can be understood as a convex relaxation of hierarchical clustering. Pairwise affinities  $\phi_{ij} > 0$  can be chosen heuristically to accelerate computation and improve empirical performance, detailed below.

Under this formulation, the number of clusters can be selected automatically as the number of unique rows in the solution matrix  $\hat{\boldsymbol{\mu}}$ . Indeed, the method entails a continuous solution path as a function of the parameter  $\gamma$  — a larger  $\gamma$  gives the fusion penalty more relative influence, resulting in fewer unique centers or clusters (Chi and Lange, 2015). Convexity ensures a unique global minimizer, suggesting stability of any valid iterative optimization algorithm regardless of initial condition. A convex formulation is also attractive from a theory perspective; works by Zhu et al. (2014); Tan and Witten (2015); Radchenko and Mukherjee (2017) provide recovery guarantees, and Chi and Steinerberger (2019) establish conditions under which, the solution path recovers a tree. Computationally, Chi and Lange (2015) provide a framework based on splitting methods that render the work of Lindsten et al. (2011) practical in a unified framework for various choices of  $q$  defining the fusion penalty norm. The idea has been extended to many related tasks including tensors, metric versions, co-clustering, multi-view and histogram-valued data. (Wu et al., 2016; Chi et al., 2018; Park et al., 2019; Wang and Allen, 2019).

Despite the recent success of convex clustering, two notable and related shortcomings include its limitations in high dimensions and its strong reliance on careful specification of affinities  $\phi_{ij}$ . Typically, users follow a recommendation that combines  $k$ -nearest neighbors ( $k$ -NN) and Gaussian kernels (Chi and Lange,

2015): that is,

$$\phi_{ij} = \mathbb{1}_{\{i,j\}}^k \exp \left\{ - \frac{\|\mathbf{x}_i - \mathbf{x}_j\|^2}{\tau} \right\} \quad (2)$$

where the indicator  $\mathbb{1}_{\{i,j\}}^k$  is equal to 1 if  $\mathbf{x}_j$  is among the  $k$ -NNs of  $\mathbf{x}_i$  with respect to  $\|\cdot\|$  and 0 otherwise, and the constant  $\tau$  is a bandwidth parameter. The success of such heuristics for choosing  $\phi_{ij}$  varies depending on the application, and improper specification may lead to pathological behavior including splits in the clustering path or abrupt merging to the overall mean (Hocking et al., 2011; Chi and Lange, 2015). Further, this Gaussian “blurring” becomes ineffective in high dimensions where pairwise Euclidean distances appearing in the kernel as well as  $k$ -NN evaluations become less informative (Aggarwal et al., 2001). Though a convex formulation ensures a unique global optimum, the instability it seeks to address is conserved in this sense: the method becomes fragile with respect to good choice of  $\phi_{ij}$  rather than initial guess.

Toward addressing high dimensionality, a sparse variant of convex clustering has been developed by Wang et al. (2018), and proposes to include an additional group lasso penalty on the *columns* of the centroid matrix as follows:

$$\min_{\boldsymbol{\mu}} \frac{1}{2} \sum_{i=1}^n \|\mathbf{x}_i - \boldsymbol{\mu}_i\|_2^2 + \gamma_1 \sum_{i < j} \phi_{ij} \|\boldsymbol{\mu}_i - \boldsymbol{\mu}_j\|_q + \gamma_2 \sum_{l=1}^p u_l \|\boldsymbol{\mu}_l\|_2. \quad (3)$$

While applying such penalties to the columns of  $\boldsymbol{\mu}$  preserves convexity, it introduces unwanted shrinkage toward the origin, and comes with higher computational costs and additional tuning parameters. Methodologically, this approach as well as extensions to convex clustering mentioned above borrow heavily from the splitting framework introduced by Chi and Lange (2015), and similarly rely on careful choice of  $\phi_{ij}$ .

The penalty formulations in convex clustering and sparse convex clustering largely borrow from techniques that have proven successful in regression (Tibshirani et al., 2005; Yuan and Lin, 2006) but do not fully leverage some of the good intuition established in the existing clustering literature. In this article, we advocate maneuvering to a *biconvex* objective, which will enable us to bridge the benefits of convex clustering to ideas that have successfully improved classical clustering schemes. Specifically, we introduce an additional optimization variable  $\mathbf{w}$  to enable feature weighing and selection. Such *feature weights* (DeSarbo et al., 1984; Modha and Spangler, 2003), have been used to improve many classical clustering schemes (de Amorim, 2016): for instance, the weighted  $k$ -means ( $W$ - $k$ -means) method (Huang et al., 2005) seeks to solve the following minimization problem:

$$\min_{\boldsymbol{\mu}, \mathbf{w}} \left\{ \sum_{i=1}^n \min_{1 \leq j \leq k} \sum_{l=1}^p w_l^2 d(x_{il}, \mu_{jl}) \right\}, \text{ subject to } \sum_{l=1}^p w_l = 1,$$

where  $\mathbf{w} = [w_1, \dots, w_p]^\top$  is the vector of non-negative feature weights modifying the usual  $k$ -means objective, and  $d(\cdot, \cdot)$  is a similarity measure typically chosen as the Euclidean norm. Variations using entropy regularization (Jing et al., 2007; Chakraborty et al., 2020b) and non-linear distance measures (De Amorim and Mirkin, 2012) have also been explored. A framework for sparse clustering by Witten and Tibshirani (2010) also employs such feature weights in seeking to maximize the between cluster sum-of-squares

$$\sum_{l=1}^p w_l \left( \frac{1}{n} \sum_{i=1}^n \sum_{i'=1}^n d(x_{il}, x_{i'l}) - \sum_{j=1}^k \frac{1}{|C_j|} \sum_{i, i' \in C_j} d(x_{il}, x_{i'l}) \right) \quad (4)$$

with respect to clusters  $C_j$ , subject to  $\ell_1$  and  $\ell_2$  constraints on weights  $\|\mathbf{w}\|_2 \leq 1$ ,  $\|\mathbf{w}\|_1 \leq s$ . We remark that feature weights should not be confused with the weight terms appearing in sparse regression techniques such as the adaptive lasso (Zou, 2006) — in particular, they are disjoint from the optimization variable and are penalized separately. Our approach will leverage this fact to allow for feature weighing and selection without excess shrinkage of the centroids toward the global mean.

These advantages come at the cost of sacrificing convexity, yet biconvex formulations inherit many of the same appealing properties such as stability and robustness compared to general non-convex problems (Gorski et al., 2007). Indeed, optimization routines for solving biconvex objectives come with attractive convergence guarantees (Tseng, 2001) and provide efficient solutions to biconvex statistical learning tasks such as non-negative matrix factorization (Lee and Seung, 2001). In contrast to the variable splitting approaches used by Wang et al. (2018); Chi and Lange (2015), we show that our objective function can be optimized directly via block-coordinate descent, reflecting the simpler alternating update form that typifies many now canonical clustering algorithms.

In addition to improving clustering performance and providing interpretable estimates feature relevance, biconvex clustering also ameliorates sensitivity to ad-hoc specifications of the affinities  $\phi_{ij}$ . As a sparse set of weights is maintained throughout the clustering task, pairwise distances and nearest neighbors can be considered within a lower-dimensional, learned feature space that *adaptively* informs  $\phi_{ij}$ . Before further detailing the proposed framework, we begin with a simple toy example to motivate our contributions.

**Motivating Example** Consider a toy dataset simulated from two ground truth clusters each with 100 associated points. The data are designed so that they can be discriminated along only the first two features. Next, we add twelve uninformative features generated from a standard normal distribution that serve only to decrease the signal-to-noise ratio. We study the results of various clustering algorithms by visualizing their solutions projected onto the two relevant dimensions. The performances of different peer algorithms are shown in Figure 1.

Our proposed method successfully recovers the ground truth (Figure 1a), while prior work that seeks a sparse solution, solves a convex relaxation, or both fail due to the large number of noise variables. We examine the performance of sparse convex clustering (Wang et al., 2018) in particular to further emphasize the effect of updating affinities by way of the learned feature weight vector. To understand why sparse convex clustering fails to recover the true cluster structure here despite attempting to perform feature selection as evident in Figure 1d, we examine a heatmap of the affinities  $\phi_{ij}$  computed under Euclidean distance as defined in (2). Figure 2a shows that because of the large relative influence of noise features, pairwise distances computed in the original Euclidean space provide only limited information, reflected in the noisy pattern of  $\phi_{ij}$  in the left panel. In contrast, updating  $\phi_{ij}$  according to (2) where distances are defined under the *learned* feature space induced by  $\mathbf{w}$  reveals clear structure (Figure 2). To further highlight this point, we may re-run sparse convex clustering provided with the affinities learned by our algorithm as inputs. The method is now able to recover

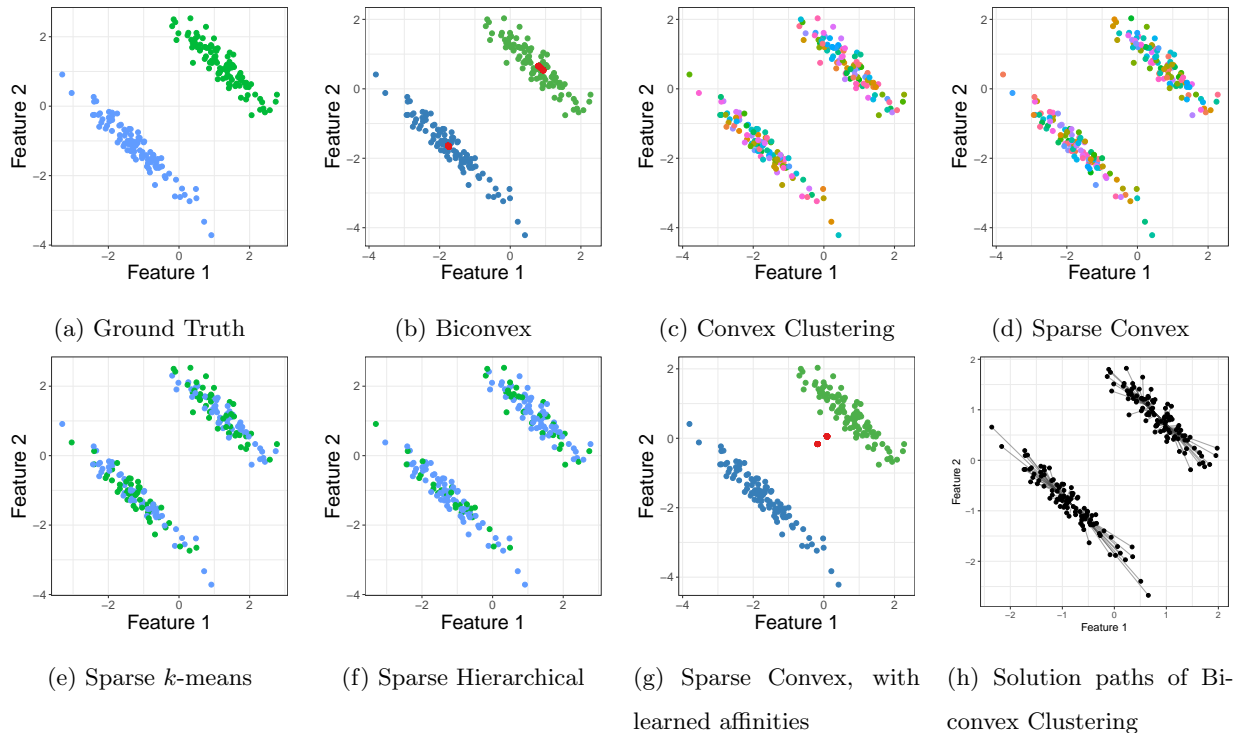


Figure 1: Performance of different peer algorithms on a toy dataset, showing the efficacy of biconvex clustering in a low signal-to-noise-ratio setting.

the ground truth, displayed in Figure 1g. Note that despite achieving a perfect clustering on this relatively simple synthetic data, the estimated centers are noticeably biased toward the origin. This behavior arises from applying shrinkage penalties directly to the centroids, and can negatively affect clustering accuracy in more realistic and challenging data settings.

The rest of the paper is organized as follows. Section 2 introduces the biconvex clustering formulation, and establishes some intuition in relation to prior work. We next derive a coordinate descent algorithm with simple, closed-form updates toward solving the resulting optimization problem with respect to the centroids and feature weights. Notably, as the feature representation adapts under the learned feature weights, users have the option to update pairwise affinities  $\phi_{ij}$  across iterations rather than rely on their *a priori* initialization throughout the clustering task. Next, the properties of the proposed method are studied closely in Section 3, where we begin by deriving finite sample prediction bounds that imply consistency of the estimates. This analysis is followed by establishing convergence of the descent method and assessing the computational complexity and practical considerations of the algorithm. These results are validated empirically in Section 4, where performance is thoroughly assessed by standard clustering metrics as well as in terms of feature selection over several simulation studies. We then apply the method to several case studies in Section 5, including a high-dimensional movement data corpus and a DNA microarray study of human leukemia, followed by discussion.

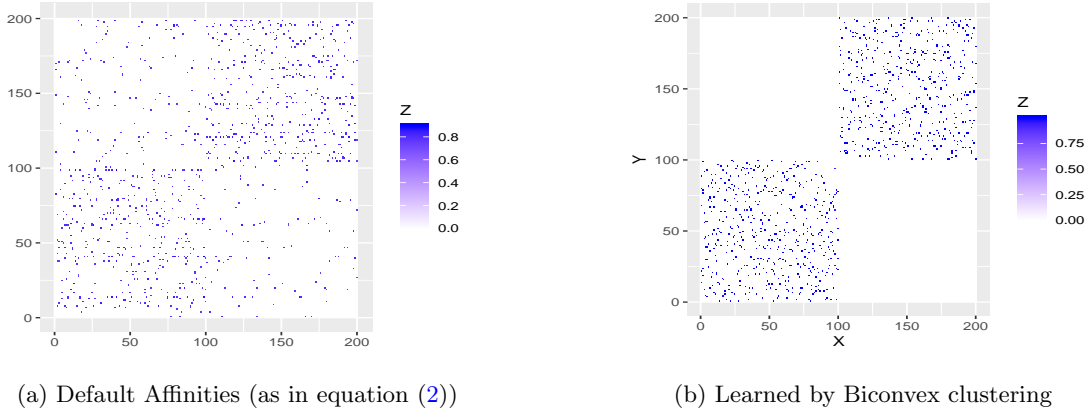


Figure 2: Heatmap of affinities  $\phi_{ij}$  show that default affinities can be misleading, while those learned by biconvex clustering reveal the cluster structure of the toy dataset.

## 2 Biconvex Clustering and adaptive feature selection

In this section, we present biconvex clustering and discuss the intuition behind the proposed formulation. We then derive a block coordinate descent algorithm for efficiently minimizing the resulting objective function.

### 2.1 Problem formulation and intuition

Let  $\mathbf{X} \in \mathbb{R}^{n \times p}$ , where the row  $\mathbf{x}_i$  contains feature values of the  $i^{\text{th}}$  data point. Consider the objective function

$$f(\boldsymbol{\mu}, \mathbf{w}) = \sum_{i=1}^n \|\mathbf{x}_i - \boldsymbol{\mu}_i\|_{\mathbf{w}}^2 + \gamma \sum_{i \neq j}^n \phi_{ij} \|\boldsymbol{\mu}_i - \boldsymbol{\mu}_j\|_2 \quad \text{subject to} \quad w_l \geq 0, \sum_{l=1}^p w_l = 1, \quad (5)$$

where the optimization variables  $(\mathbf{w}, \boldsymbol{\mu})$  denote the vector of feature weights and an  $n \times p$  matrix whose rows contain the centroids, respectively. For a vector  $\mathbf{y} \in \mathbb{R}^p$ , we define the norm induced by  $\mathbf{w}$  as  $\|\mathbf{y}\|_{\mathbf{w}}^2 := \sum_{l=1}^p (w_l^2 + \lambda w_l) y_l^2$ . We see that the first component  $\sum_{i=1}^n \|\mathbf{x}_i - \boldsymbol{\mu}_i\|_{\mathbf{w}}^2$  of (5) assesses the fit between the centroids  $\boldsymbol{\mu}$  and the data  $\mathbf{X}$  measured in a way that is weighed by  $\mathbf{w}$  (Huang et al., 2005). Note that if we fix all  $w_l \propto 1$  throughout,  $\|\mathbf{y}\|_{\mathbf{w}}$  becomes a scalar multiple of the Euclidean norm  $\|\mathbf{y}\|_2$ , and thus minimizing (5) is equivalent to convex clustering as a special case. Like convex clustering, the procedure begins with  $n$  centroids—one at each data point—which merge toward each other due to the term  $\sum_{i < j}^n \|\boldsymbol{\mu}_i - \boldsymbol{\mu}_j\|_2$ . It is straightforward to show that the solution path is unique and depends continuously on  $\gamma$  (Chi and Lange, 2015).

This objective is convex in either of the optimization variables as the other is held fixed: that is, it is *biconvex* in  $(\boldsymbol{\mu}, \mathbf{w})$ . To establish some intuition, we focus on the variable  $\boldsymbol{\mu}$  and fix all  $w_l = 1/p$  now for exposition. Recall for sufficient  $\gamma$ , the fusion penalty encourages centroids to merge so that only a subset of the rows of  $\boldsymbol{\mu}$  are unique; denote this resulting set of centers as  $\mathbf{C} \in \mathbb{R}^{k \times d}$ . As a result of merging, the

measure of fit term

$$\sum_{i=1}^n \|\mathbf{x}_i - \boldsymbol{\mu}_i\|_2^2 \quad \text{gradually tends to} \quad \sum_{i=1}^n \min_j \|\mathbf{x}_i - \mathbf{C}_j\|_2^2. \quad (6)$$

The familiar quantity on the right hand side appears in classic formulations such as  $k$ -means, and is equivalent to the within-cluster variance (Lloyd, 1982). Now removing the restriction  $w_l = 1/p$ , reveals how our formulation improves upon existing continuous clustering methods. The weights  $\mathbf{w}$  enable us to learn which features are helpful for distinguishing these clusters: fixing  $\boldsymbol{\mu}$  and expanding the measure of fit yields

$$\sum_{i=1}^n \sum_{l=1}^p (w_l^2 + \lambda w_l) (x_{il} - \mu_{il})^2.$$

Under the simplex constraint  $\sum_{l=1}^p w_l = 1$ , the  $\lambda w_l$  term promotes sparsity—screening out irrelevant features—while without the  $w_l^2$  term, the linear cost in  $w$  under the sum constraint would assign all weight to the most important feature and result in a degenerate solution (Witten and Tibshirani, 2010). Thus the objective in  $\mathbf{w}$  entails feature weighing as well as selection. With  $\boldsymbol{\mu}$  fixed, the terms  $\sum_{i=1}^n (x_{il} - \mu_{il})^2 := u_l$  that had played the role of the objective when optimizing  $\boldsymbol{\mu}$  now act as “weights” themselves to inform the optimization of  $\mathbf{w}$ . To again relate to the familiar within-cluster variance, we can rewrite

$$\sum_{i=1}^n \min_j \|\mathbf{x}_i - \mathbf{C}_j\|_2^2 = \sum_{l=1}^p \tilde{u}_l, \quad \text{where we define} \quad \tilde{u}_l = \sum_{i=1}^n \mathbb{1}_{\{i,j\}} (x_{i,l} - C_{j,l})^2; \quad (7)$$

here  $\mathbb{1}_{\{i,j\}}$  is an indicator function of whether data point  $i$  is closest (assigned) to center  $j$ . As the  $\boldsymbol{\mu}_i$  terms coalesce via the fusion penalty and approach a set of unique centers  $\mathbf{C}$ , our definition of  $u_l$  coincides with this familiar interpretation under equal  $w_l$ . We see that  $u_l$  can thus be interpreted as the total contribution along dimension  $l$  to within-cluster variance across clusters; this is related to the dispersion measures used by Friedman and Meulman (2004).

In other words, a large  $u_l$  indicates that feature  $l$  is less useful toward discriminating clusters, and promotes setting  $w_l$  to zero. Further note that upon making the change of variables  $z_l = w_l/u_l$ , the unit simplex constraint  $\sum_{l=1}^p w_l = 1$  on  $\mathbf{w}$  can now be reinterpreted as a *weighted simplex* in  $\mathbf{z}$ . Intuitively, this means that distances to activating constraints are driven by the learned cluster information rather than static. This adaptive behavior expands upon prior work on sparse clustering (Witten and Tibshirani, 2010; Wang et al., 2018) and imports intuition behind the celebrated adaptive lasso for regression (Zou, 2006). Where these related ideas in regression entail two-stage estimation procedures, our framework allows for  $\mathbf{w}, \boldsymbol{\mu}$  to be learned *jointly*.

Before proceeding with the optimization method, we make some remarks regarding fusion penalties of the form  $\sum_{i < j} \|\boldsymbol{\mu}_i - \boldsymbol{\mu}_j\|_q$ . Historically, the namesake *fusion* is borrowed from an unpublished technical report (Land and Friedman, 1997) which explores variable fusion under penalties on a vector  $\boldsymbol{\nu}$  of the form

$$\|\nu_j - \nu_{j-1}\|_q^\alpha. \quad (8)$$

A prominent example is the fused lasso or total variation penalty  $\sum_{j=2}^p \|\nu_j - \nu_{j-1}\|_1$  (Tibshirani et al., 2005) for seeking local constancy when  $\boldsymbol{\nu}$  is a vector of ordered regression coefficients by promoting sparsity in  $\boldsymbol{\nu}$

as well as its successive differences. Tibshirani et al. (2005) mention they do not consider other values of  $\alpha$  in (8) because piecewise constant coefficient solutions under  $\alpha = 1$  are desirable and easily interpretable in their context. Other natural choices such as  $\alpha = 2$  have appeared much less frequently in the literature in contexts such as precision estimation (Hebiri et al., 2011; Price et al., 2015; Lam et al., 2016). When such exact sparsity is not the end goal, however, such alternate choices may produce the desired behavior yet yield more elegant solutions. We will argue that this is the case in our present context.

The following sections show that squaring the norms appearing in the fusion penalty will confer substantial computational advantages. This slight “ridge fusion” modification entails the resulting objective

$$f(\boldsymbol{\mu}, \mathbf{w}) = \sum_{i=1}^n \|\mathbf{x}_i - \boldsymbol{\mu}_i\|_{\mathbf{w}}^2 + \gamma \sum_{i \neq j}^n \phi_{ij} \|\boldsymbol{\mu}_i - \boldsymbol{\mu}_j\|_2^2 \quad \text{subject to} \quad w_l \geq 0, \sum_{l=1}^p w_l = 1, \quad (9)$$

which now encourages centroids to merge toward each other by way of penalizing the *quadratic* variation between row pairs of  $\boldsymbol{\mu}$  rather than the total variation distance. Doing so no longer results in exact merging—subsets of rows now agglomerate closely rather than coalescing to a single point. Though the resulting cluster assignment under a naïve interpretation would be trivial—each point is assigned to its own centroid—we demonstrate how to obtain a nontrivial clustering from the solution to (9) analogous to that under exact merging in Section 3.2. In particular, assigning clusters as so shares the same worst-case complexity as simply reading off the unique rows of the solution under (5).

## 2.2 Optimization

This section derives closed form coordinate descent updates for the subproblems in  $\boldsymbol{\mu}$  and  $\mathbf{w}$ . We begin by rewriting objective (9), expanding and decomposing the first term into two components as written below (still subject to the simplex constraint on  $\mathbf{w}$ ):

$$f(\boldsymbol{\mu}, \mathbf{w}) = \sum_{i=1}^n \sum_{l=1}^p w_l^2 (x_{il} - \mu_{il})^2 + \gamma \sum_{i,j=1;i \neq j}^n \sum_{l=1}^p \phi_{ij} (\mu_{il} - \mu_{jl})^2 + \lambda \sum_{l=1}^p w_l \sum_{i=1}^n (x_{il} - \mu_{il})^2. \quad (10)$$

The block coordinate descent updates for minimizing the objective (10) are given by the solutions to the following two subproblems:

- *Problem P<sub>1</sub>*: Fix  $\mathbf{w} = \mathbf{w}_0$ , minimize  $f(\boldsymbol{\mu}, \mathbf{w}_0)$  w.r.t.  $\boldsymbol{\mu}$ .
- *Problem P<sub>2</sub>*: Fix  $\boldsymbol{\mu} = \boldsymbol{\mu}_0$ , minimize  $f(\boldsymbol{\mu}_0, \mathbf{w})$  w.r.t.  $\mathbf{w}$ , subject to  $\sum_{l=1}^p w_l = 1; w_l \geq 0$ .

Let us solve *Problem P<sub>1</sub>*. First, observe that if  $w_l = 0$ , one can simply choose  $\mu_{il} = 0$  for all  $i \in \{1, \dots, n\}$  in order to decrease the value of the objective function. Thus take  $w_l > 0$ ; differentiating the objective function with respect to  $\mu_{il}$ , we obtain

$$\mu_{il} = \frac{\gamma \sum_{i \neq j} \phi_{ij} \mu_{jl} + \gamma \sum_{i \neq j} \phi_{ji} \mu_{ji} + w_l^2 x_{il} + \lambda w_l x_{il}}{\gamma \sum_{i \neq j} \phi_{ij} + \gamma \sum_{i \neq j} \phi_{ji} + w_l^2 + \lambda w_l}. \quad (11)$$

Fixing  $\boldsymbol{\mu}$ , the minimization of  $\mathbf{w}$  is summarized below, with more details of its derivation in the Appendix.

**Theorem 1.** *The solution to Problem  $P_2$  is given by*

$$w_l^* = \frac{1}{2} S\left(\frac{\alpha^*}{\sum_{i=1}^n (x_{il} - \mu_{il})^2}, \lambda\right) \quad (12)$$

where for any  $y \geq 0$ , and  $x \in \mathbb{R}$ ,  $S(x, y)$  denotes the soft thresholding function defined

$$S(x, y) = \begin{cases} x - y & \text{if } x \geq y \\ x + y & \text{if } x \leq -y \\ 0 & \text{Otherwise.} \end{cases}$$

and  $\alpha^*$  satisfies the equation  $\sum_{l=1}^p \frac{1}{2} S\left(\frac{\alpha}{\sum_{i=1}^n (x_{il} - \mu_{il})^2}, \lambda\right) = 1$ .

In particular, solutions to each of the subproblems are parameter-separated; that is, all computations can be carried out component-wise, and the univariate problems can be executed in parallel.

---

**Algorithm 1** Biconvex Clustering algorithm (BCC)

---

**Input:**  $\mathbf{X} \in \mathbb{R}^{n \times p}$ ,  $\lambda > 0$ ,  $\gamma > 0$       **Output:**  $\boldsymbol{\mu}$

**Step 0.** Initialize  $\boldsymbol{\mu} = \mathbf{X}$ ,  $w_l = 1/p$ ,  $l = 1, \dots, p$ , and

(optional)  $\phi_{ij} = \exp\{-\|\mathbf{x}_i - \mathbf{x}_j\|_2^2\} \mathbb{1}_{\{j \in k\text{-NN of } i \text{ under } \|\cdot\|_2\}}$      $i = 1, \dots, n; l = 1, \dots, p$ .

**repeat**

**Step 1.** Update  $\boldsymbol{\mu}$  (coordinate-separable, can be parallelized) by

$$\mu_{il} \leftarrow \frac{\gamma \sum_{i \neq j} \phi_{ij} \mu_{jl} + \gamma \sum_{i \neq j} \phi_{ji} \mu_{jl} + w_l^2 x_{il} + \lambda w_l x_{il}}{\gamma \sum_{i \neq j} \phi_{ij} + \gamma \sum_{i \neq j} \phi_{ji} + w_l^2 + \lambda w_l}.$$

**Step 2.** Update  $\alpha^*$  satisfying  $\sum_{l=1}^p S\left(\frac{\alpha}{\sum_{i=1}^n (x_{il} - \mu_{il})^2}, \lambda\right) = 2$  (i.e. via univariate bisection).

**Step 3.** Update  $\mathbf{w}$  (coordinate-separable, can be parallelized) by

$$w_l \leftarrow \frac{1}{2} S\left(\frac{\alpha}{\sum_{i=1}^n (x_{il} - \mu_{il})^2}, \lambda\right).$$

**Step 4.** (Optional) Update

$$\phi_{ij} = \exp\{-\|\mathbf{x}_i - \mathbf{x}_j\|_{\mathbf{w}/p}^2\} \mathbb{1}_{\{j \in k\text{-NN of } i \text{ under } \|\cdot\|_{\mathbf{w}}\}} \quad i = 1, \dots, n; l = 1, \dots, p.$$

**until** convergence criterion based on objective (10) is reached

---

Before analyzing the properties and complexity of the proposed method, we pause to discuss notable differences from prior work. Recall the sparse convex clustering objective (3) addresses high-dimensionality through penalizing the columns of the centroid matrix  $\boldsymbol{\mu}$  directly. This approach is intuitive and nicely preserves convexity in the overall objective. However, the formulation can introduce significant shrinkage to the origin, an effect that may lead to bias as well as spurious selection. Computationally, the solution method in sparse convex clustering modifies the same two approaches outlined in Chi and Lange (2015),

namely sparse variants of the alternating minimization (AMA) and alternating directions (ADMM) methods. Computation becomes more complicated, however: one step within the alternating directions method requires an additional iterative algorithm of fitting  $p$  group lasso regressions in the simplest case when  $q = 2$ . Perhaps more troubling is that not only do the two implementations S-AMA and S-ADMM differ in speed, but may lead to quite different clustering solutions (Wang et al., 2018). The stability properties that convex formulations originally aimed to provide thus do not carry over. In contrast, our biconvex formulation can be solved via alternating between simple solutions to each subproblem given by (11) and (12). A return to form reflecting the structure of classic methods such as Lloyd’s algorithm, the proposed method marks a departure from the majority of existing work on convex clustering and its variants, which rely on variable splitting that entail additional dual variables and step-size selection. This affords us a transparent and efficient block coordinate descent method, summarized in Algorithm 1. We establish convergence guarantees, finite sample bounds that imply consistency, and desirable computational properties in the following section.

### 3 Convergence and statistical properties

This section establishes the theoretical properties of the (global) optimal solutions of the proposed objective function by providing finite sample bounds on the prediction error. We also analyze the computational cost of biconvex clustering and discuss its convergence properties.

#### 3.1 Finite sample bounds and prediction consistency

We begin by analyzing statistical properties of the biconvex clustering technique by providing the finite sample error bounds for the prediction error. In particular, these bounds provide sufficient conditions for consistency of the centroid and weight estimates.

Subject to the simplex constraint on  $\mathbf{w}$ , recall the biconvex clustering objective

$$\min_{\boldsymbol{\mu}, \mathbf{w}} \left\{ \sum_{i=1}^n \|\mathbf{x}_i - \boldsymbol{\mu}_i\|_{\mathbf{w}}^2 + \gamma \sum_{i \neq j} \|\boldsymbol{\mu}_i - \boldsymbol{\mu}_j\|_2^2 \right\}. \quad (13)$$

Throughout this section, we will assume that  $\phi_{ij}$  are kept fixed and for clarity of exposition will proceed after vectorizing the problem setup. To this end let  $\mathbf{x} = \text{vec}(\mathbf{X})$  and  $\mathbf{u} = \text{vec}(\boldsymbol{\mu})$ , where  $\text{vec}(\cdot)$  denotes the function that flattens a matrix by appending its columns together. Now  $\mathbf{x}, \mathbf{u} \in \mathbb{R}^{np}$ , with  $\mathbf{x}_{(i-1)p+j} = X_{ij}$  and  $\mathbf{u}_{(i-1)p+j} = \mu_{ij}$ . Similarly, let  $\mathbf{W} = \text{diag}(w_1^2 + \lambda w_1, \dots, w_p^2 + \lambda w_p) \otimes \mathbf{I}_p$ , where  $\otimes$  denotes the Kronecker product. To deal with the penalty term, let  $\mathbf{D} \in \mathbb{R}^{[p \frac{n(n-1)}{2}] \times np}$  be such that  $\mathbf{D}_{\mathcal{C}(i,j)} = \boldsymbol{\mu}_i - \boldsymbol{\mu}_j$ , where  $\mathcal{C}(i, j)$  is an index set: then the optimization problem (13) can now be rewritten as

$$\min_{\mathbf{u} \in \mathbb{R}^{np}} \left\{ (\mathbf{x} - \mathbf{u})^\top \mathbf{W} (\mathbf{x} - \mathbf{u}) + \gamma \sum_{i < j} \|\mathbf{D}\mathbf{u}\|_2^2 \right\}. \quad (14)$$

Our finite sample bounds will follow from imposing that errors are sub-Gaussian, as reasonable assumption satisfied by many parametric distributions. Before we proceed, we will require the following lemma by

Hanson and Wright (1971).

**Lemma 1.** (Hanson and Wright, 1971) Let  $\mathbf{z}$  be a vector of independent sub-Gaussian random variables with mean zero and variance  $\sigma^2$ . Let  $\mathbf{M}$  be a symmetric matrix. Then, there exists some constants  $c_1, c_2 > 0$  such that for any  $t > 0$ ,

$$P(\mathbf{z}^\top \mathbf{M} \mathbf{z} \geq t + \text{tr}(\mathbf{M})) \leq \exp \left\{ - \min \left( \frac{c_1 t^2}{\sigma^4 \|\mathbf{M}\|_F}, \frac{c_2 t}{\sigma^2 \|\mathbf{M}\|_{sp}} \right) \right\},$$

where,  $\|\cdot\|_F$  and  $\|\cdot\|_{sp}$  denotes the Frobenius and spectral norms respectively.

We now are ready to establish the following theorem providing a finite sample bound on the prediction error, denoting the constant  $\gamma' = \frac{\gamma}{np}$ .

**Theorem 2.** Suppose  $\mathbf{x} = \mathbf{u} + \boldsymbol{\epsilon}$ , where,  $\boldsymbol{\epsilon} \in \mathbb{R}^{np}$  is a vector of independent sub-gaussian random variables, with mean 0 and variance  $\sigma^2$ . Let  $\hat{\mathbf{u}}$  and  $\hat{\mathbf{W}}$  be the solutions minimizing (14). Then for  $\gamma' > 2\sigma(1 + \lambda)\sqrt{\frac{\log(p\binom{n}{2})}{np}}$ , the bound

$$\frac{1}{2np} \|\hat{\mathbf{u}} - \mathbf{u}\|_{\hat{\mathbf{W}}}^2 \leq \sigma^2(1 + \lambda) \left[ \frac{1}{n} + \sqrt{\frac{\log(np)}{n^2 p}} \right] + \gamma'(1 - \frac{1}{n}) + \frac{\gamma'}{n} \sum_{i \neq j} \|\mathbf{D}_{C(i,j)} \mathbf{u}\|_2 + \gamma' \sum_{i \neq j} \|\mathbf{D}_{C(i,j)} \mathbf{u}\|^2$$

holds with probability at least  $1 - \frac{2}{p\binom{n}{2}} - \exp \left( - \min \left\{ c_1 \log(np), \frac{c_2}{3} \sqrt{p \log(np)} \right\} \right)$ .

The complete details of the proof are provided in the Appendix. We pause to examine the result and discuss its implications. We see from Theorem 2 that the average prediction error is bounded by oracle terms

$$\gamma'(1 - \frac{1}{n}) + \frac{\gamma'}{n} \sum_{i \neq j} \|\mathbf{D}_{C(i,j)} \mathbf{u}\|_2 + \gamma' \sum_{i \neq j} \|\mathbf{D}_{C(i,j)} \mathbf{u}\|^2.$$

Note the first summand tends to 0 as  $n, p \rightarrow \infty$ ; thus, consistency of estimates follow whenever  $\gamma'(1 - \frac{1}{n}) + \frac{\gamma'}{n} \sum_{i \neq j} \|\mathbf{D}_{C(i,j)} \mathbf{u}\|_2 + \gamma' \sum_{i \neq j} \|\mathbf{D}_{C(i,j)} \mathbf{u}\|^2 = o(1)$ . Regarding when the oracle terms are  $o(1)$ : suppose  $p > n$  and there exists a fixed number of distinguishing features. In this setting,  $\|\mathbf{D}_{C(i,j)} \mathbf{u}\| = O(1)$ , and so  $\sum_{i \neq j} \|\mathbf{D}_{C(i,j)} \mathbf{u}\|_2$  as well as  $\sum_{i \neq j} \|\mathbf{D}_{C(i,j)} \mathbf{u}\|^2$  are  $O(n^2)$ . This implies that our method is prediction consistent whenever  $\sqrt{\frac{n^3 \log(p\binom{n}{2})}{p}} = o(1)$ . We see that up to a logarithmic factor, it is sufficient that  $n = o(p^{\frac{1}{3}})$  for the condition to hold, which we may expect in sufficiently high-dimensional settings.

### 3.2 Convergence and complexity analysis

Here we examine the algorithmic aspects of biconvex clustering, beginning with its convergence in finite number of iterations.

**Theorem 3.** Within a finite number of steps, Algorithm 1 converges to a coordinate-wise minimum of (9).

*Proof.* Let  $g_t$  be the value of the objective function (9) at iteration  $t$ . From the update steps of Algorithm 1, it is clear that  $g_{t+1} \leq g_t$ , for all  $t \in \mathbb{N}$ . Thus the sequence  $\{g_t\}_{t=1}^\infty$  is forms a decreasing sequence, and

moreover  $g_t \geq 0, \forall t \in \mathbb{N}$ . Thus  $\{g_t\}_{t=1}^\infty$  converges by the monotone convergence theorem. Thus, for all  $\epsilon > 0$ , there exists  $T \in \mathbb{N}$ , such that  $g_T - g_{T+1} \leq \epsilon$ , so that an absolute or relative convergence criterion based on (9) is satisfied in finite iterations. Because the objective is biconvex, applying Theorem 5.1 of Tseng (2001) immediately implies that the limit point is a coordinate-wise minimum of (9).

□

**Complexity** We now examine the computational cost of the proposed method. Evaluating  $\mu_{il}$  in step 1 takes  $\mathcal{O}(k)$  steps where  $k$  is the number of nonzero summands, i.e. number of nonzero  $\phi_{ij}$  coefficients. Since there are  $n \times p$  many computations, it takes  $\mathcal{O}(npk)$  time to complete the centroid updates, which can be executed in parallel. Computing  $\sum_{i=1}^n (x_{il} - \mu_{il})^2$  requires  $\mathcal{O}(n)$  time for each  $l = 1, \dots, p$ , contributing  $\mathcal{O}(np)$  total, while solving for  $\alpha^*$  via bisection is  $\mathcal{O}(p)$ , as is the soft-threshold update of  $\mathbf{w}$ . Therefore, the overall per-iteration complexity of the algorithm is  $\mathcal{O}(npk + np + p) = \mathcal{O}(npk)$ . Note for vanilla convex clustering, the computational complexity is  $\mathcal{O}(n^2p)$  for ADMM and  $\mathcal{O}(npk)$  for AMA, where  $k$  is also quadratic in  $n$  in the worst case. Thus we are able to either match or improve upon its complexity despite handling the additional task of variable weighing and selection simultaneously.

**Cluster assignments from  $\mu$**  Convex clustering promotes centroids to merge at convergence, but one must “read off” the unique rows of a matrix  $\mathbf{V}$  containing all difference pairs appearing in the penalty term to make cluster assignments. Doing so calls breadth-first search (BFS) to identify connected components of the graph induced by  $\mathbf{V}$  (Chi and Lange, 2015), which has linear complexity in the cardinality of the edge set plus the vertex set  $\mathcal{O}(|\mathcal{E}| + |\mathcal{V}|) = \mathcal{O}(n^2)$ . Recall that squaring the penalty term in our approach does not lead to exact coalescence of centroids; in place of BFS, we instead determine cluster assignments from  $\mu$  by a dynamic tree cut (Langfelder et al., 2008) on the resulting dendrogram. The bottleneck computation involves creating a distance matrix, which also has  $\mathcal{O}(n^2)$  complexity but is trivially parallelizable. Even though our algorithm does not rely on exact fusion of centroids, the assignment step in our algorithm does not entail higher computational cost. The efficacy of this approach is demonstrated in Section 4.

**Nearest neighbor affinities** When users apply the optional Step 4, Algorithm 1 allows for affinities  $\phi_{ij}$  to adapt with the learned feature space. Existing approaches to convex clustering have been criticized for their strong dependence on choice of  $\phi$ , which remain fixed throughout the algorithm and strongly influence performance. Under dense choice of  $\phi$ , clusters may not merge until the trivial solution at the origin, and convex clustering may perform worse than standard  $k$ -means (Tan and Witten, 2015). Further computational considerations arise, for instance in choosing step-sizes within splitting methods based on the eigenvalues of the Laplacian associated with the edge set  $\mathcal{E}$  induced by  $\phi$ . Our algorithm can take advantage of the same recommended heuristics for initializing  $\phi$ , but allow for these *a priori* choices to correct throughout the task by recomputing all distances under the induced norm  $\|\cdot\|_{\mathbf{w}}$  as the estimate for  $\mathbf{w}$  improves. The merits of this adaptivity, which occurs in Step 4 of Algorithm 1, are investigated empirically in the following section.

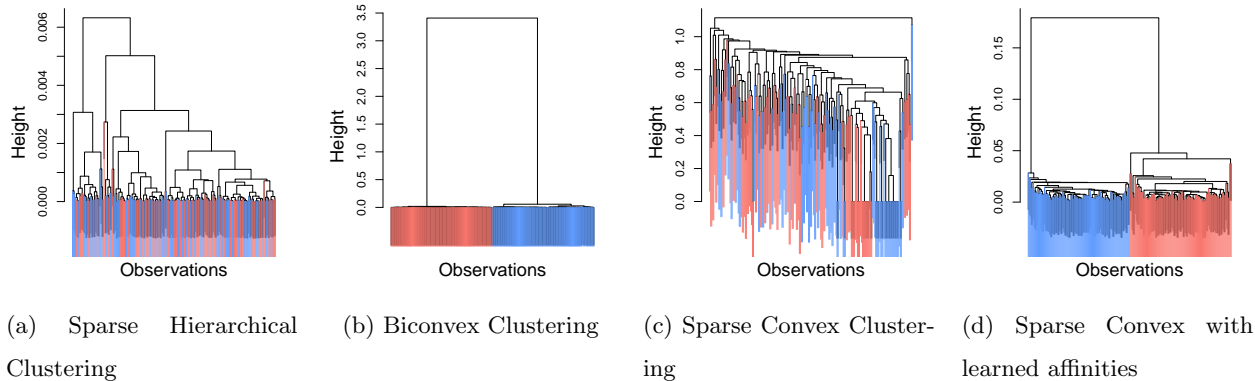


Figure 3: Dendrograms for solutions to motivating example (Sec. 1). Identifying the two true clusters via a tree cut is straightforward, while competing methods are sensitive to choice of cut height.

## 4 Simulation studies

In this section, we examine several performance aspects of the proposed method. Before comparing the feature selection and clustering accuracy between biconvex clustering and peer methods, we highlight the reduced reliance on sensitivity to heuristic specification of  $\phi_{ij}$ . To this end, we revisit the simple motivating example from Section 1 and examine the dendrograms produced under various settings. Figure 3 displays the resulting dendrograms obtained under peer algorithms from the motivating example, showing that the height of the branches corresponding to correct separation into the two true clusters is markedly larger under our approach than the competitors. This clear separation suggests that any reasonable choice of dynamic tree cut provides a stable way to convert the solution  $\hat{\mu}$  to accurate cluster assignments. We do not observe this to be the case when examining dendrograms of competing sparse clustering methods. When initializing the competing sparse convex clustering approach using our learned affinities  $\phi_{ij}$  induced by  $\hat{w}$  (discussed further below), the dendrogram structure under the competing approach is largely corrected, though still visibly more sensitive to choice of tree cut than our method. Under both settings for choice of  $\phi_{ij}$ , sparse convex clustering did not lead to exact merging despite the  $\ell_1$  penalty on columns; thus its solutions are also visualized as dendrograms rather than applying breadth-first search to identify unique rows of the centroid matrix.

Next, we take a closer look at the effect of various choices of  $\phi_{ij}$  on performance in a controlled setting. We consider a simulated dataset in a fairly low signal-to-noise regime, with ambient dimension  $p = 200$  but only 5 features relevant to clustering, and  $n = 50$  observations. The data are visualized using t-SNE in the first panel of Figure 4a. Panel (b) shows that when updating affinities  $\phi_{ij}$  with the choice of  $k = 5$  nearest neighbors, biconvex clustering produces an estimate whose dendrogram clearly reveals the true structure. In contrast to convex clustering and its existing variants, this remains true even without sparsifying the affinities via  $k$ -nearest neighbors: that is, setting  $k = n$  so that the neighbor graph is dense, panel (c) reveals that the relative height of the dendrogram that corresponds to a perfect recovery of the four true clusters is

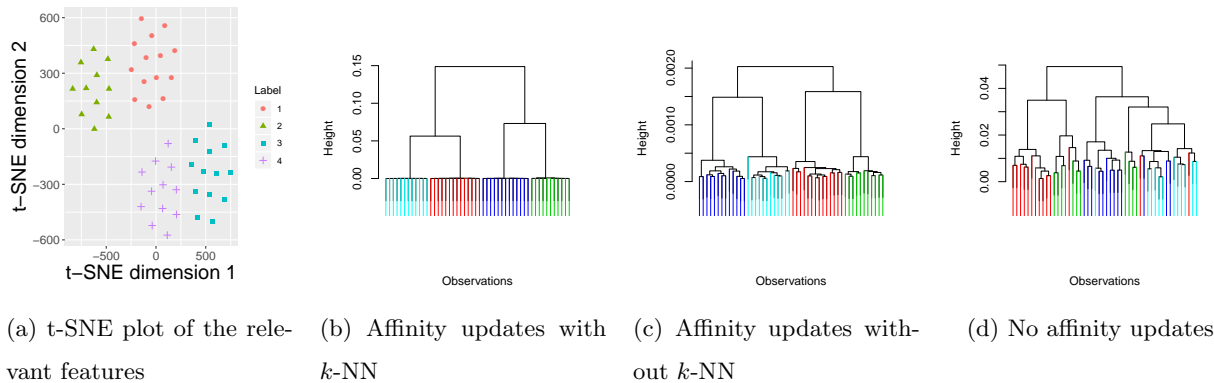


Figure 4: Dendrograms produced by biconvex clustering with and without affinity updates, showing that the best result is obtained when the affinities  $\phi_{ij}$  are updated using  $k$ -NN (with  $k = 5$ ).

again very pronounced. Finally, we consider biconvex clustering without any affinity updates; the final plot color coded with the ground truth is shown in Figure 4 (d), which now fails to perfectly recover the true partition. This study highlights the robustness of our method to heuristic choices in  $\phi_{ij}$ —the algorithm produces dendrograms that are able to reveal the ground truth whether or not we sparsify the choice of affinities. At the same time, the example demonstrates the power of adapting within the learned feature space, without which it is not possible to cut the dendrogram and obtain the true clustering.

We next consider several simulation studies that more closely examine the merits of biconvex clustering empirically in terms of feature selection accuracy and clustering accuracy.

#### 4.1 Feature selection

The following simulation examines feature selection performance of our method compared to the widely used sparse  $k$ -means clustering method of [Witten and Tibshirani \(2010\)](#). Our simulation study begins with  $n = 1000$ ,  $p = 100$  and  $k = 5$ . The matrix  $\Theta_{k \times p}$  whose rows contain the true cluster centroids is generated as follows:

1. Simulate  $\theta_{j,l} \sim Unif(0, 1)$  for all  $j = 1, \dots, k$  and  $l = 1, \dots, 5$ .
2. Set  $\theta_{j,l} = 0$  for all  $l \notin \{1, \dots, 5\}$  and all  $j$ .

After obtaining  $\Theta$ , we generate data  $\mathbf{X}$  so that only the first 5 features are informative toward distinguishing clusters, simulated as follows:

$$x_{il} \sim \frac{1}{k} \sum_{j=1}^k \mathcal{N}(\theta_{j,l}, 0.015) \text{ if } l \in \{1, \dots, 5\};$$

$$x_{il} \sim \mathcal{N}(0, 1) \text{ if } l \notin \{1, \dots, 5\}.$$

We standardize all features and repeat the simulation to generate 30 simulated datasets. We compare results under biconvex clustering with tuning parameters  $\lambda = 0.2$  and  $\gamma = 100$ , and sparse  $k$ -means with parameter

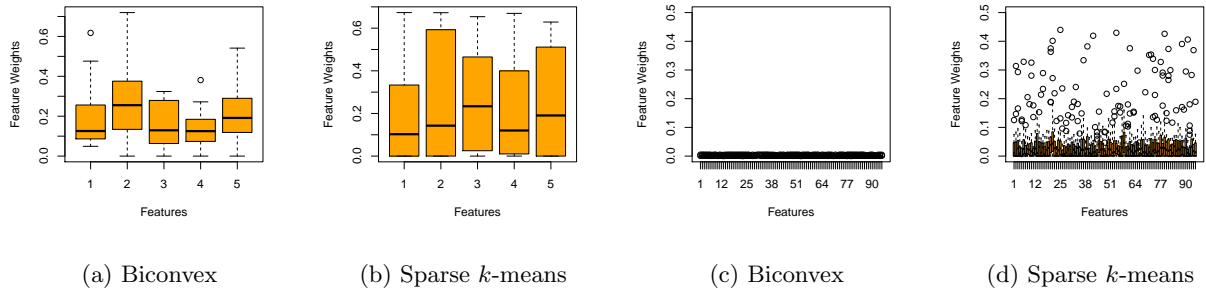


Figure 5: Figures 5a and 5b show the boxplots of the feature weights for the 5 relevant features for biconvex clustering and sparse  $k$ -means respectively. Figures 5c and 5d show the same for the 95 irrelevant features. Biconvex clustering consistently zeroes out the irrelevant features. Sparse  $k$ -means fails to do so while frequently assigning nonzero weights to noise variables.

$s^*$  selected using the gap statistic (Tibshirani et al., 2001) over a fine grid of 100 values of  $s \in [1.01, 10]$ , using the R package `sparcl`.

Boxplots of the resulting feature weights obtained under both algorithms, separated by relevant and irrelevant features, are displayed in Figure 5. From panels 5a and 5c, we see that biconvex clustering consistently assigns weight to all 5 relevant features, while correctly zeroing out the remaining irrelevant features. On the other hand, while Sparse  $k$ -means assigns a large chunk of weight to the relevant features (Figure 5b), there is much more variance across datasets. More to the point, Figure 5d shows that sparse  $k$ -means fails to consistently zero out irrelevant dimensions, often assigning them weight values on par with the relevant features. Finally, though our formulation loses convexity, we observe that in practice the method is quite insensitive to initial guess. We extend this simulation study in the Appendix, demonstrating that solutions remain stable to random initializations of  $w$ .

## 4.2 Clustering accuracy

Having seen that our method is more stable in terms of feature selection in the previous simulation study, we now shift attention to examine the quality of clusterings produced by the various peer algorithms more closely. Non-convex objective functions such as those based on  $k$ -means are known to become increasingly susceptible to poor local minima when the number of clusters grows (Lloyd, 1982; Xu and Lange, 2019). Here we show that our biconvex formulation enjoys robustness to this phenomenon compared to competing nonconvex approaches. On the other hand, though we can no longer guarantee that solutions are necessarily global minimizers, our method delivers more accurate solutions than convex clustering and its sparse counterpart. Our empirical studies indicates that this tradeoff is well worth it, and suggests that when the convex relaxation may be far from the original formulation for which it serves as proxy, its global solution may not translate to desirable clustering performance.

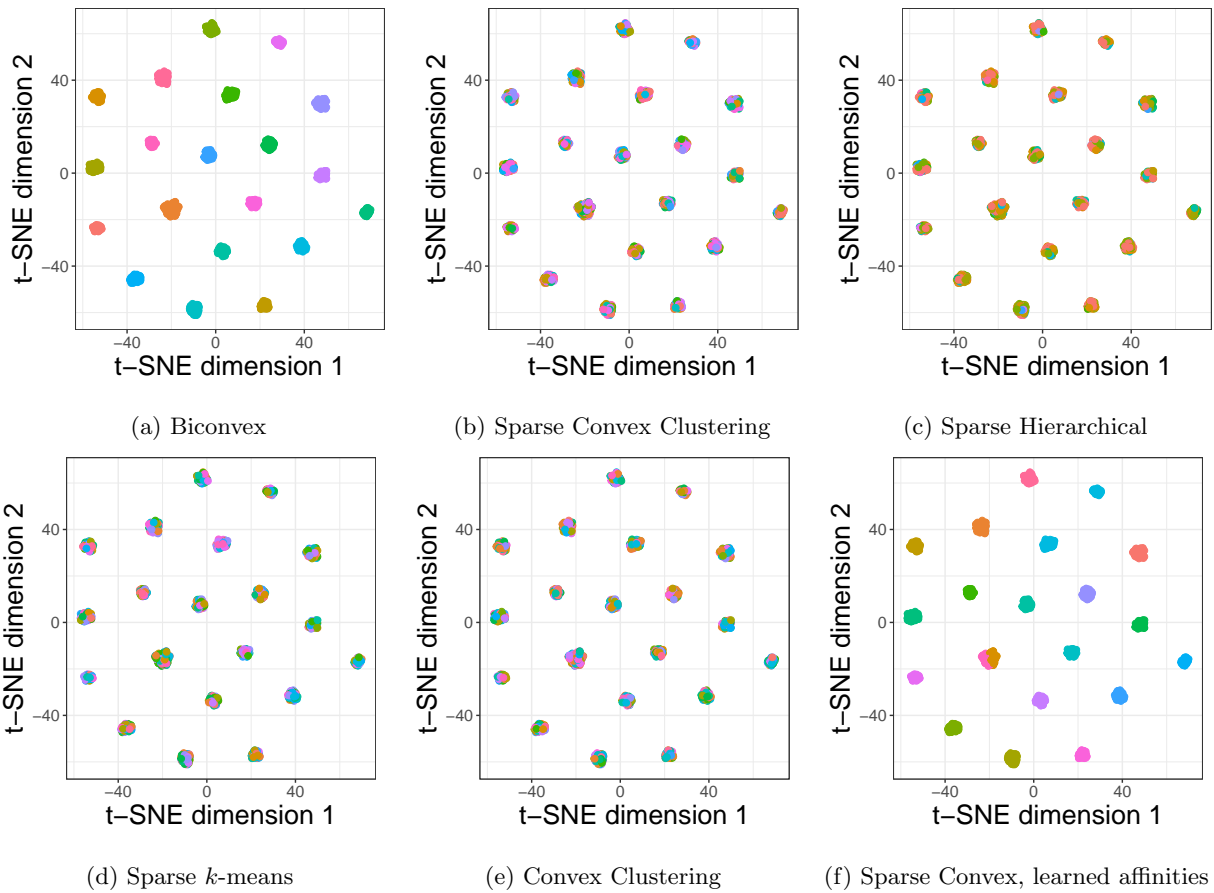


Figure 6:  $t$ -SNE plots showing the performance of the peer algorithms when the number of clusters is high in a sparse clustering scenario.

To illustrate this claim empirically, we simulate data as in Section 4.1 but increase the number of clusters to  $k = 20$ . The performance (best performance out of 20 independent runs for sparse  $k$ -means and sparse hierarchical clustering) of the peer algorithms are shown in Figure 6, plotted using  $t$ -Stochastic Neighbourhood Embedding ( $t$ -SNE) (Maaten and Hinton, 2008). Cconvex clustering, sparse convex clustering, and the sparse variants of  $k$ -means and hierarchical clustering are all implemented using their respective R packages. Sparse  $k$ -means tends to deteriorate when it is trapped by a poor local optimum of the objective function, which becomes highly non-convex when  $k$  is large. Convex clustering unsurprisingly fails because it is not designed for high-dimensional scenarios where many of the features contain no information about the cluster structure of the data.

The poor performance of sparse convex clustering (Wang et al., 2018) may arise largely due to the strong dependence on choice of the affinity parameters, since the signal-to-noise-ratio is quite low and the selection of nearest neighbours is significantly influenced by the irrelevant dimensions. To assess this suspicion, we try sparse convex clustering again under the *learned* affinities resulting from the estimate  $\hat{\mathbf{w}}$  obtained by biconvex clustering. Indeed, Figure 6f shows that the performance of sparse convex clustering is rescued when provided with  $\hat{\phi}_{ij}$  defined with respect to the weighted feature space induced by  $\hat{\mathbf{w}}$ . Finally, the solution under our biconvex clustering method is identical to the ground truth partition, plotted in Figure 6a. Not shown in the plot, biconvex clustering also assigns positive feature weights to only the true discriminative features. The resulting dendrogram are displayed in Figure 9 of the Appendix, which provides further insight validating this claim. Due to differences in implementation, we do not include a detailed runtime comparison. We note however that even a naive implementation of biconvex clustering runs significantly faster than convex clustering and sparse convex clustering.

### 4.3 Performance with increasing feature dimension

This simulation study aims to assess the performance of biconvex clustering and competitors as the number of non-informative features increases. The first two features are drawn from four bivariate Gaussian distributions with means at  $(\pm 1, \pm 1)$  with equal probability; these corners of the cube with side length 2 can be thought of as the true centers along the first two dimensions. The remaining  $d$  features are uninformative, drawn from a standard normal distribution; we will examine performance as  $d$  increases.

We run each algorithm 20 times as the number of noise variables  $d$  varies from 0 to 30. The average performance of each peer methods are shown in Figure 7. Biconvex clustering perfectly recovers the ground truth clustering of the data for all values of  $d$ , which is perhaps unsurprising given the simple ground truth structure. However, the average performance of the other competing algorithms deteriorate noticeably as the number of noise variables increases, performing almost as poorly as random assignment at  $d = 30$ . It should be noted that biconvex clustering remains effective even in regimes as the signal-to-noise-ratio continues to drop, yielding perfect clustering when  $d = 100$  (not shown) in this simulation setting.

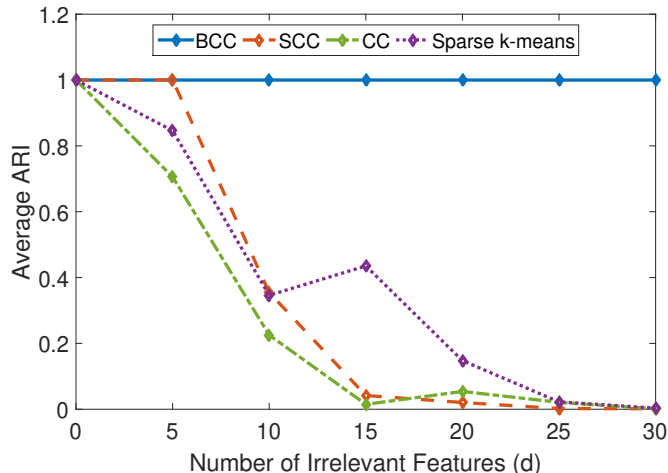


Figure 7: Performance of different peer algorithms in a low signal-to-noise ratio setting as the number of irrelevant features increases (Section 4.3). Here SCC, BCC, CC denote the Sparse Convex Clustering, Biconvex Clustering and Convex Clustering, respectively.

## 5 Case studies

We turn our attention to several case studies. On these real datasets, we evaluate performance of the algorithms via the Adjusted Rand Index (ARI) (Hubert and Arabie, 1985) between the output partition and the ground truth. An ARI value of 1 indicates perfect clustering whereas a value of 0 indicates complete mismatch between the ground truth and the partition obtained by the algorithm.

### 5.1 Movement data

We begin by analyzing the Libras movement data corpus, which consists of 15 classes each containing 24 observations. Each class represents a hand movement type, and observations are described via 90 features representing the coordinates of movement. The data are publicly available (Dua and Graff, 2017) and a subset of the full dataset was chosen to showcase the sparse convex clustering algorithm Wang et al. (2018), enabling us to consider a conservative comparison to prior work.

We normalize all features before clustering, and following Wang et al. (2018), we use 6 movement types for evaluation purposes, chosen to avoid excess overlap among some highly correlated classes. Each of the peer algorithms is tuned and run using their recommended settings, as implemented in their respective R packages. We run all sparse  $k$ -means variants from 20 initial guesses and report the best performing trial. The hyperparameters of convex and sparse convex clustering are selected using the stability selection procedure outlined by Fang and Wang (2012).

We apply biconvex clustering with  $\lambda = 0.2$  and  $\gamma = 100$  and use the `dynamicTreeCut` package in R to assign cluster labels to the resulting centroid estimates (Langfelder et al., 2008). The partition we obtain is

Table 1: Feature selection and clustering performance, Libras movement data.

Algorithm	# Nonzero Weights	# Clusters	ARI
Sparse $k$ -means	83	6	0.46
Sparse Hierarchical Clustering	14	6	0.11
Average Linkage	90	4	0.36
Convex Clustering	90	8	0.61
Sparse Convex Clustering (S-AMA)	63	3	0.31
Sparse Convex Clustering (S-ADMM)	13	3	0.31
Biconvex Clustering	90	5	<b>0.79</b>

shown in Figure 8d. We also run the average linkage algorithm on the dataset, again using `dynamicTreeCut` on the data, as well as sparse convex clustering algorithm using S-AMA (Wang et al., 2018) and sparse  $k$ -means clustering (Witten and Tibshirani, 2010). The solutions are visualized in Figure 8, and the ARI values obtained from the peer algorithms are displayed shown in Table 1. We see that the difference in performance between the proposed method and existing competitors is clear. Interestingly, we find that biconvex clustering does not zero out any features in this case, though proper feature weighing clearly helps it to uncover the true cluster structure in the dataset.

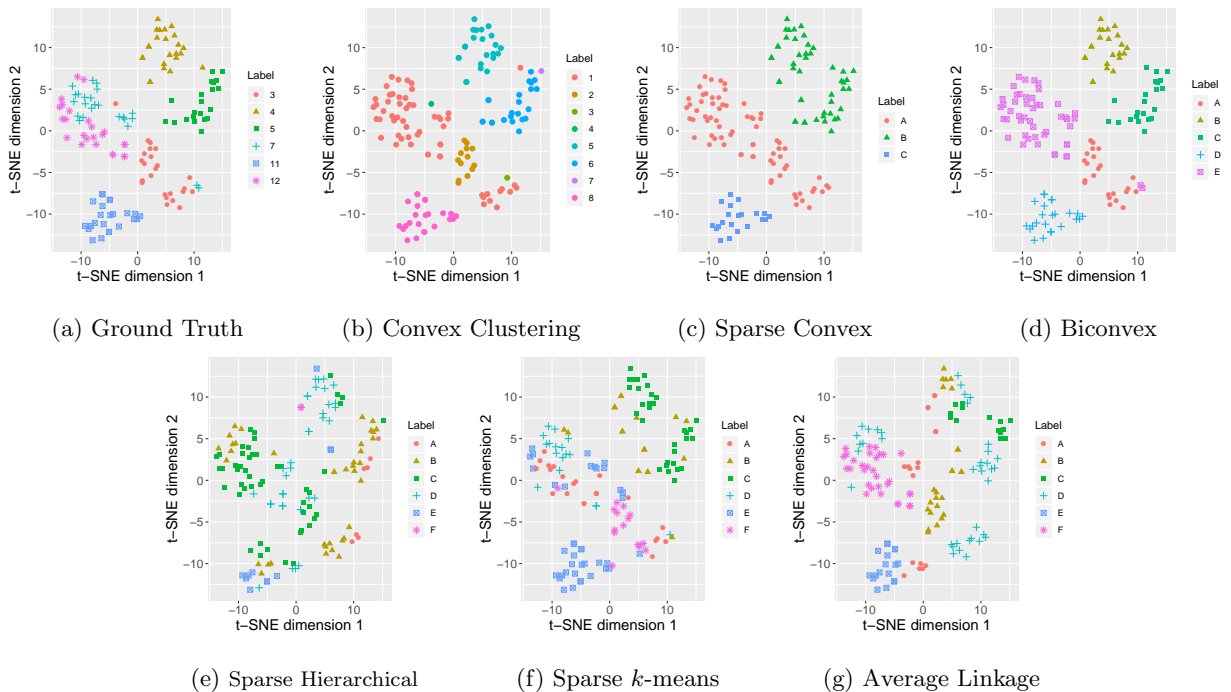


Figure 8: Comparison of solutions in t-SNE embedding, Libras dataset.

## 5.2 Leukemia data

We next revisit a classic DNA microarray dataset from a study of leukemia on human subjects. The data are collected and described by [Golub et al. \(1999\)](#) and after a standard preprocessing, consist of 3571 gene expression levels collected over 72 samples (comprised of 62 bone marrow samples and 10 from the peripheral blood). Out of the 72 samples, 47 correspond to acute lymphoblastic leukemia (ALL) and 25 to acute myeloblastic leukemia (AML). The observations are centered and scaled before use.

To distinguish between these two classes on the basis of gene expression, we apply biconvex clustering with hyperparameters  $\lambda = 0.01$  and  $\gamma = 0.1$ . At convergence, our method selects 456 relevant genes among the original space of 3571 features, and is able to correctly classify all but one one point. Prior work has suggested that this point is likely a potential outlier ([Chakraborty et al., 2020a](#)). In this case study, we emphasize the success of gene selection in addition to recovering the ground truth partition almost perfectly. Among 50 genes that were deemed potentially relevant to distinguishing between leukemias in the original study by [Golub et al. \(1999\)](#), 46 are also selected by our algorithm. A later study by [Chow et al. \(2001\)](#) revisits the data with a focus on identifying the discriminative genes, employing heuristic criteria based on a mix of three relevance measures: a naive Bayes score, a median vote, and mean aggregate relevance. These measures are combined in a supervised learning framework based on Support Vector Machines (SVMs) that requires true labels as inputs. They reported that the top 50 genes under each of the relevance measures had little overlap; we find all genes in the intersection of the three criteria are selected by our method. In particular, the genes deemed most significant in this prior study— Adipsin (M84526) and Cystatin C (M27891)— were assigned the 3rd and 7th largest feature weights among the 456 selected by biconvex clustering. While findings from neither of these previous studies should be taken as ground truth, it is reassuring that their results are consistent with our feature selection results. Though it is perhaps unsurprising that our method may outperform those applied to these data at that time— these studies predated the sparse clustering framework of [Witten and Tibshirani \(2010\)](#)—our simultaneous clustering and feature weighing method offers new insights in a reexamination of the data. A detailed list of the top 20 genes identified by our method is included in [Table 2](#), and visualization of solutions via t-SNE is provided in [Figure 11](#) of the Appendix.

## 6 Discussion

The proposed methodology seeks to address three chief challenges in clustering: high-dimensionality via feature weighing and selection, sensitivity to initialization via a biconvex formulation, and selection of cluster centers via a penalty formulation that encourages centroids to agglomerate along the solution path. Biconvex clustering can be seen as occupying a middle ground between the convex clustering objective and the original non-convex objective arising from hierarchical clustering. We build upon recent algorithmic developments for convex clustering and its variants, bridging these insights to good intuition established in the classical clustering literature.

Gene ID	Gene Annotation	Feature Weight
D88270_at	pre-B lymphocyte gene 1, VPREB1	0.008134539
D88422_at	Cystatin A	0.010030157
M11722_at	Terminal transferase mRNA	0.007699765
M23197_at	CD33 antigen (differentiation antigen)	0.010011479
M27891_at	CST3 Cystatin C (amyloid angiopathy and cerebral hemorrhage)	0.012265694
M28826_at	CD1B antigen (thymocyte antigen)	0.050758810
M63138_at	CTSD Cathepsin D (lysosomal aspartyl protease)	0.007746540
M84526_at	DF D component of complement (adipsin)	0.014803023
M89957_at	IGB Immunoglobulin-associated beta (B29)	0.008915087
U05259_rna1_at	MB-1 gene	0.010192411
U46499_at	Gluthanione S-Transferase, Microsoma	0.013318948
X04145_at	CD3G antigen, gamma polypeptide (TiT3 complex)	0.010848832
X14975_at	GB DEF5CD1 R2 gene for MHC-related antigen	0.011330957
X58529_at	Immunoglobulin mu, part of exon 8	0.009955146
X87241_at	HFat protein	0.012668398
X95735_at	Zyxin	0.009213922
Z15115_at	TOP2B Topoisomerase (DNA) II beta (180kD)	0.009112349
M13560_s_at	Probable Protein Disulfide Isomerase ER-60 Precursor	0.008775355
X76223_s_at	GB DEF5MAL gene exon 4	0.015623870
M31523_at	TCF3 Transcription factor 3	0.013837447
	(E2A immunoglobulin enhancer binding factors E12/E47)	

Table 2: Top 20 genes identified by biconvex clustering on leukemia dataset, along with their gene IDs, annotations and feature weights.

Not only does feature selection reduce dimension while retaining interpretability of the features (compared to a generic dimension reduction pre-processing step), but feature weights obtained by the algorithm improve clustering quality while serving as informative and interpretable quantities themselves. Our algorithm returns simple alternating updates that resemble classical clustering algorithms, while conferring several advantages over traditional approaches. In particular, we show that sacrificing convexity and exact coalescence of centroids enables algorithmic and theoretical benefits that we consider well worth the tradeoff. Fruitful avenues for future work include extending the framework to tensor settings (Sun and Li, 2019), and exploring other optimization frameworks such as semi-smooth Newton (Yuan et al., 2018; Sun et al., 2018) and stochastic descent algorithms (Panahi et al., 2017) that may lead to further computational gains. Similar penalties involving  $k$ -NN affinities within a fusion penalty have recently been studied for non-parametric regression (Madrid Padilla et al., 2020). Similar to their benefits in our setting, the  $k$ -NN terms enable “manifold adaptivity”, in addition to the fusion term which provides local adaptivity. It will be fruitful to explore the extent to which our contributions are useful in related contexts such as regression and trend filtering, as well as to potentially import their theoretical insights into the clustering setting.

## References

- Aggarwal, C. C., Hinneburg, A., and Keim, D. A. (2001). On the surprising behavior of distance metrics in high dimensional space. In *International Conference on Database Theory*, pages 420–434. Springer.
- Bachem, O., Lucic, M., Hassani, H., and Krause, A. (2016). Fast and provably good seedings for k-means. In *Advances in Neural Information Processing Systems*, pages 55–63.
- Chakraborty, S. and Das, S. (2019). A strongly consistent sparse  $k$ -means clustering with direct  $l_1$  penalization on variable weights. *arXiv preprint arXiv:1903.10039*.
- Chakraborty, S., Paul, D., and Das, S. (2020a). Hierarchical clustering with optimal transport. *Statistics & Probability Letters*, page 108781.
- Chakraborty, S., Paul, D., Das, S., and Xu, J. (2020b). Entropy weighted power k-means clustering. In *International Conference on Artificial Intelligence and Statistics*, pages 691–701.
- Chi, E. C., Gaines, B. R., Sun, W. W., Zhou, H., and Yang, J. (2018). Provable convex co-clustering of tensors. *arXiv preprint arXiv:1803.06518*.
- Chi, E. C. and Lange, K. (2015). Splitting methods for convex clustering. *Journal of Computational and Graphical Statistics*, 24(4):994–1013.
- Chi, E. C. and Steinerberger, S. (2019). Recovering trees with convex clustering. *SIAM Journal on Mathematics of Data Science*, 1(3):383–407.

- Chow, M., Moler, E., and Mian, I. (2001). Identifying marker genes in transcription profiling data using a mixture of feature relevance experts. *Physiological Genomics*, 5(2):99–111.
- de Amorim, R. C. (2016). A survey on feature weighting based k-means algorithms. *Journal of Classification*, 33(2):210–242.
- De Amorim, R. C. and Mirkin, B. (2012). Minkowski metric, feature weighting and anomalous cluster initializing in k-means clustering. *Pattern Recognition*, 45(3):1061–1075.
- DeSarbo, W. S., Carroll, J. D., Clark, L. A., and Green, P. E. (1984). Synthesized clustering: A method for amalgamating alternative clustering bases with differential weighting of variables. *Psychometrika*, 49(1):57–78.
- Dua, D. and Graff, C. (2017). UCI Machine Learning Repository.
- Fang, Y. and Wang, J. (2012). Selection of the number of clusters via the bootstrap method. *Computational Statistics & Data Analysis*, 56(3):468–477.
- Friedman, J. H. and Meulman, J. J. (2004). Clustering objects on subsets of attributes (with discussion). *Journal of the Royal Statistical Society: Series B (Statistical Methodology)*, 66(4):815–849.
- Golub, T. R., Slonim, D. K., Tamayo, P., Huard, C., Gaasenbeek, M., Mesirov, J. P., Coller, H., Loh, M. L., Downing, J. R., Caligiuri, M. A., et al. (1999). Molecular classification of cancer: class discovery and class prediction by gene expression monitoring. *Science*, 286(5439):531–537.
- Gorski, J., Pfeuffer, F., and Klamroth, K. (2007). Biconvex sets and optimization with biconvex functions: a survey and extensions. *Mathematical Methods of Operations Research*, 66(3):373–407.
- Hamerly, G. and Elkan, C. (2004). Learning the k in k-means. In *Advances in Neural Information Processing Systems*, pages 281–288.
- Hanson, D. L. and Wright, F. T. (1971). A bound on tail probabilities for quadratic forms in independent random variables. *The Annals of Mathematical Statistics*, 42(3):1079–1083.
- Hebiri, M., Van De Geer, S., et al. (2011). The smooth-lasso and other  $\ell_1 + \ell_2$ -penalized methods. *Electronic Journal of Statistics*, 5:1184–1226.
- Hocking, T. D., Joulin, A., Bach, F., and Vert, J.-P. (2011). Clusterpath: An algorithm for clustering using convex fusion penalties. In *Proceedings of the 28th International Conference on International Conference on Machine Learning, ICML’11*, page 745–752, Madison, WI, USA. Omnipress.
- Huang, J. Z., Ng, M. K., Hongqiang Rong, and Zichen Li (2005). Automated variable weighting in k-means type clustering. *IEEE Transactions on Pattern Analysis and Machine Intelligence*, 27(5):657–668.

- Hubert, L. and Arabie, P. (1985). Comparing partitions. *Journal of classification*, 2(1):193–218.
- Jain, A. K. (2010). Data clustering: 50 years beyond k-means. *Pattern Recognition Letters*, 31(8):651–666.
- Jing, L., Ng, M. K., and Huang, J. Z. (2007). An entropy weighting k-means algorithm for subspace clustering of high-dimensional sparse data. *IEEE Transactions on Knowledge and Data Engineering*, 19(8):1026–1041.
- Lam, K. Y., Westrick, Z. M., Müller, C. L., Christiaen, L., and Bonneau, R. (2016). Fused regression for multi-source gene regulatory network inference. *PLoS Computational Biology*, 12(12):e1005157.
- Land, S. R. and Friedman, J. H. (1997). Variable fusion: A new adaptive signal regression method. Technical report, Technical Report 656, Department of Statistics, Carnegie Mellon University . . . .
- Langfelder, P., Zhang, B., and Horvath, S. (2008). Defining clusters from a hierarchical cluster tree: the dynamic tree cut package for R. *Bioinformatics*, 24(5):719–720.
- Lee, D. D. and Seung, H. S. (2001). Algorithms for non-negative matrix factorization. In *Advances in Neural Information Processing Systems*, pages 556–562.
- Lindsten, F., Ohlsson, H., and Ljung, L. (2011). Clustering using sum-of-norms regularization: With application to particle filter output computation. In *2011 IEEE Statistical Signal Processing Workshop (SSP)*, pages 201–204. IEEE.
- Lloyd, S. (1982). Least squares quantization in PCM. *IEEE Transactions on Information Theory*, 28(2):129–137.
- Maaten, L. v. d. and Hinton, G. (2008). Visualizing data using t-SNE. *Journal of Machine Learning Research*, 9(Nov):2579–2605.
- MacQueen, J. et al. (1967). Some methods for classification and analysis of multivariate observations. In *Proceedings of the fifth Berkeley symposium on mathematical statistics and probability*, volume 1, pages 281–297. Oakland, CA, USA.
- Madrid Padilla, O. H., Sharpnack, J., Chen, Y., and Witten, D. M. (2020). Adaptive nonparametric regression with the k-nearest neighbour fused lasso. *Biometrika*, 107(2):293–310.
- Modha, D. S. and Spangler, W. S. (2003). Feature weighting in k-means clustering. *Machine Learning*, 52(3):217–237.
- Ostrovsky, R., Rabani, Y., Schulman, L. J., and Swamy, C. (2013). The effectiveness of Lloyd-type methods for the k-means problem. *Journal of the ACM (JACM)*, 59(6):1–22.

- Panahi, A., Dubhashi, D., Johansson, F. D., and Bhattacharyya, C. (2017). Clustering by sum of norms: Stochastic incremental algorithm, convergence and cluster recovery. In *International Conference on Machine Learning*, pages 2769–2777.
- Park, C., Choi, H., Delcher, C., Wang, Y., and Yoon, Y. J. (2019). Convex clustering analysis for histogram-valued data. *Biometrics*, 75(2):603–612.
- Pelckmans, K., De Brabanter, J., Suykens, J. A., and De Moor, B. (2005). Convex clustering shrinkage. In *PASCAL Workshop on Statistics and Optimization of Clustering Workshop*.
- Price, B. S., Geyer, C. J., and Rothman, A. J. (2015). Ridge fusion in statistical learning. *Journal of Computational and Graphical Statistics*, 24(2):439–454.
- Radchenko, P. and Mukherjee, G. (2017). Convex clustering via  $\ell_1$  fusion penalization. *Journal of the Royal Statistical Society: Series B (Statistical Methodology)*, 79(5):1527–1546.
- Sun, D., Toh, K.-C., and Yuan, Y. (2018). Convex clustering: Model, theoretical guarantee and efficient algorithm. *arXiv preprint arXiv:1810.02677*.
- Sun, W. W. and Li, L. (2019). Dynamic tensor clustering. *Journal of the American Statistical Association*, pages 1–28.
- Tan, K. M. and Witten, D. (2015). Statistical properties of convex clustering. *Electronic journal of statistics*, 9(2):2324.
- Tibshirani, R., Saunders, M., Rosset, S., Zhu, J., and Knight, K. (2005). Sparsity and smoothness via the fused lasso. *Journal of the Royal Statistical Society: Series B (Statistical Methodology)*, 67(1):91–108.
- Tibshirani, R., Walther, G., and Hastie, T. (2001). Estimating the number of clusters in a data set via the gap statistic. *Journal of the Royal Statistical Society: Series B (Statistical Methodology)*, 63(2):411–423.
- Tropp, J. A. (2006). Just relax: Convex programming methods for identifying sparse signals in noise. *IEEE Transactions on Information Theory*, 52(3):1030–1051.
- Tseng, P. (2001). Convergence of a block coordinate descent method for nondifferentiable minimization. *Journal of Optimization Theory and Applications*, 109(3):475–494.
- Wang, B., Zhang, Y., Sun, W. W., and Fang, Y. (2018). Sparse convex clustering. *Journal of Computational and Graphical Statistics*, 27(2):393–403.
- Wang, M. and Allen, G. I. (2019). Integrative generalized convex clustering optimization and feature selection for mixed multi-view data. *arXiv preprint arXiv:1912.05449*.
- Witten, D. M. and Tibshirani, R. (2010). A framework for feature selection in clustering. *Journal of the American Statistical Association*, 105(490):713–726.

- Wu, T., Benson, A. R., and Gleich, D. F. (2016). General tensor spectral co-clustering for higher-order data. In *Advances in Neural Information Processing Systems*, pages 2559–2567.
- Xu, J. and Lange, K. (2019). Power k-means clustering. In Chaudhuri, K. and Salakhutdinov, R., editors, *Proceedings of the 36th International Conference on Machine Learning*, volume 97 of *Proceedings of Machine Learning Research*, pages 6921–6931, Long Beach, California, USA. PMLR.
- Yuan, M. and Lin, Y. (2006). Model selection and estimation in regression with grouped variables. *Journal of the Royal Statistical Society: Series B (Statistical Methodology)*, 68(1):49–67.
- Yuan, Y., Sun, D., and Toh, K.-C. (2018). An efficient semismooth Newton based algorithm for convex clustering. In *International Conference on Machine Learning*, pages 5718–5726.
- Zhu, C., Xu, H., Leng, C., and Yan, S. (2014). Convex optimization procedure for clustering: theoretical revisit. In *Advances in Neural Information Processing Systems*, pages 1619–1627.
- Zou, H. (2006). The adaptive lasso and its oracle properties. *Journal of the American Statistical Association*, 101(476):1418–1429.

# Appendix

## A Proof of Theorem 1

We now discuss the solution of the optimization problem  $P_2$ , defined in Section 2.2. Since  $\boldsymbol{\mu}$  is kept fixed in this subproblem, we define the constant  $D_l = \sum_{i=1}^n (x_{il} - \mu_{il})^2$  for brevity. Thus  $f(\boldsymbol{\mu}, \boldsymbol{w})$  (equation (10)) can be written as

$$g(\boldsymbol{w}) = \sum_{l=1}^p (w_l^2 + \lambda w_l) D_l + (\text{constant in } \boldsymbol{w}). \quad (15)$$

Equation (15) is to be minimized subject to the constraints  $\sum_{l=1}^p w_l = 1$  and  $w_l \geq 0$ , for all  $l = 1, \dots, p$ . We write the Lagrangian for this problem as follows:

$$\mathcal{L} = \sum_{l=1}^p (w_l^2 + \lambda w_l) D_l - \alpha \left( \sum_{l=1}^p w_l - 1 \right) - \sum_{l=1}^p \xi_l w_l$$

From the Karush-Kuhn-Tucker (KKT) conditions of optimality, we have,

$$\frac{\partial \mathcal{L}}{\partial w_l} = 0, \quad \forall l = 1, \dots, p. \quad (16)$$

$$\sum_{l=1}^p w_l = 1. \quad (17)$$

$$w_l \geq 0, \quad \forall l = 1, \dots, p. \quad (18)$$

$$\xi_l \geq 0. \quad (19)$$

$$\xi_l w_l = 0, \quad \forall l = 1, \dots, p. \quad (20)$$

Equation (16) implies that

$$w_l = \frac{1}{2} \left( \frac{\alpha + \xi_l}{D_l} - \lambda \right) \quad (21)$$

We now consider the following cases.

**Case 1:**  $\frac{\alpha}{D_l} > \lambda$ : Since  $\xi_l \geq 0$ , we conclude from equation (21) that  $w_l > 0$ . Thus, from equation (20), we deduce that  $\xi_l = 0$ . Plugging in this value in equation (21), we get that  $w_l = \frac{1}{2} \left( \frac{\alpha}{D_l} - \lambda \right)$ .

**Case 2:**  $\frac{\alpha}{D_l} \leq \lambda$ : Suppose  $w_l > 0$ : then equation (20) implies that  $\xi_l = 0$ . Thus, from equation (21), we would have  $w_l = \frac{1}{2} \left( \frac{\alpha}{D_l} - \lambda \right) \leq 0$ , which is a contradiction. Thus, in this case, we must have  $w_l = 0$ .

We now observe that since  $\lambda, D_l \geq 0$ , we may conclude that  $\alpha > 0$ . Otherwise, case 2 would always occur implying  $w_l = 0, \forall l = 1, \dots, p$ , which violates equation (17). Thus, case 1 holds and the slack variables  $\xi_l = 0$ . Together with equation (21), we observe that  $w_l = \frac{1}{2} S\left(\frac{\alpha}{D_l}, \lambda\right)$ . Moreover, together with constraint (17), we observe that  $\alpha$  must satisfy the equation:

$$\frac{1}{2} S\left(\frac{\alpha}{D_l}, \lambda\right) = 1.$$

This concludes the proof.

## B Proof of Theorem 2

**Theorem 2** Suppose  $\mathbf{x} = \mathbf{u} + \boldsymbol{\epsilon}$ , where,  $\boldsymbol{\epsilon} \in \mathbb{R}^{np}$  is a vector of independent sub-gaussian random variables, with mean 0 and variance  $\sigma^2$ . Suppose that  $\hat{\mathbf{u}}$  and  $\hat{W}$  are obtained from minimizing (14), then if  $\gamma' > 2\sigma(1 + \lambda)\sqrt{\frac{\log(p\binom{n}{2})}{np}}$

$$\frac{1}{2np}\|\hat{\mathbf{u}} - \mathbf{u}\|_{\hat{W}}^2 \leq \sigma^2(1 + \lambda)\left[\frac{1}{n} + \sqrt{\frac{\log(np)}{n^2p}}\right] + \gamma(1 - \frac{1}{n}) + \frac{\gamma'}{n}\sum_{i \neq j}\|D_{C(i,j)}\mathbf{u}\|_2 + \gamma'\sum_{i \neq j}\|D_{C(i,j)}\mathbf{u}\|^2$$

holds with probability at least  $1 - \frac{2}{p\binom{n}{2}} - \exp\left(-\min\left\{c_1 \log(np), \frac{c_2}{3}\sqrt{p \log(np)}\right\}\right)$ .

*Proof.* Let  $D = A\Lambda V_\beta$  be the singular value decomposition (SVD) of  $D$ . Here  $V_\beta \in \mathbb{R}^{np \times p(n-1)}$ . We can construct  $V_\alpha \in \mathbb{R}^{np \times p}$  such that  $V = [V_\alpha, V_\beta]$  is an  $np \times np$  orthonormal matrix. Thus,  $V^\top V = VV^\top = I$  and  $V_\alpha^\top V_\beta = 0$ .

Let  $\boldsymbol{\beta} = V_\beta \mathbf{u}$  and  $\boldsymbol{\alpha} = V_\alpha \mathbf{u}$ . Suppose  $\gamma' = \frac{\gamma}{np}$ . Thus the optimization problem (14) becomes

$$\min_{\boldsymbol{\alpha}, \boldsymbol{\beta}, W} \frac{1}{2np}(\mathbf{x} - V_\alpha \boldsymbol{\alpha} - V_\beta \boldsymbol{\beta})^\top W(\mathbf{x} - V_\alpha \boldsymbol{\alpha} - V_\beta \boldsymbol{\beta}) + \gamma' \sum_{i \neq j} \|D\mathbf{u}\|_2^2 \quad (22)$$

Let,  $\hat{\boldsymbol{\alpha}}, \hat{\boldsymbol{\beta}}, \hat{W}$  be the minimizers of (22). We first observe that  $\hat{\mathbf{u}} = V_\alpha \hat{\boldsymbol{\alpha}} + V_\beta \hat{\boldsymbol{\beta}}$ . Let  $Z = A\Lambda$ . To simplify notations, we write  $\|\mathbf{y}\|_{\hat{W}}^2 = \mathbf{y}^\top W \mathbf{y}$ . By definition, we have

$$\frac{1}{2np}\|(\mathbf{x} - V_\alpha \hat{\boldsymbol{\alpha}} - V_\beta \hat{\boldsymbol{\beta}})\|_{\hat{W}}^2 + \gamma' \sum_{i \neq j} \|Z\hat{\boldsymbol{\beta}}\|_2^2 \leq \frac{1}{2np}\|(\mathbf{x} - V_\alpha \boldsymbol{\alpha} - V_\beta \boldsymbol{\beta})\|_{\hat{W}}^2 + \gamma' \sum_{i \neq j} \|Z\boldsymbol{\beta}\|_2^2 \quad (23)$$

Substituting  $\mathbf{x}$  by  $\mathbf{u} + \boldsymbol{\epsilon}$ , we get,

$$\frac{1}{2np}\|V_\alpha(\hat{\boldsymbol{\alpha}} - \boldsymbol{\alpha}) + V_\beta(\hat{\boldsymbol{\beta}} - \boldsymbol{\beta})\|_{\hat{W}}^2 + \gamma' \sum_{i \neq j} \|Z\hat{\boldsymbol{\beta}}\|_2^2 \leq \frac{1}{np}G(\hat{\boldsymbol{\alpha}}, \hat{\boldsymbol{\beta}}, \hat{W}) + \gamma' \sum_{i \neq j} \|Z\boldsymbol{\beta}\|_2^2, \quad (24)$$

where,  $G(\hat{\boldsymbol{\alpha}}, \hat{\boldsymbol{\beta}}, \hat{W}) = \boldsymbol{\epsilon}^\top \hat{W}(V_\alpha(\hat{\boldsymbol{\alpha}} - \boldsymbol{\alpha}) + V_\beta(\hat{\boldsymbol{\beta}} - \boldsymbol{\beta}))$ . Since  $\hat{\boldsymbol{\alpha}}$  is the minimizer of (22), we can choose  $\hat{\boldsymbol{\alpha}}$  such that  $\mathbf{x} - V_\beta \hat{\boldsymbol{\beta}} - V_\alpha \hat{\boldsymbol{\alpha}} = 0$ . Thus we can choose  $\hat{\boldsymbol{\alpha}}$  such that,

$$\begin{aligned} \hat{\boldsymbol{\alpha}} &= V_\alpha^\top (\mathbf{x} - V_\beta \hat{\boldsymbol{\beta}}) \\ &= V_\alpha^\top (\mathbf{u} + \boldsymbol{\epsilon} - V_\beta \hat{\boldsymbol{\beta}}) = \boldsymbol{\alpha} + V_\alpha^\top \boldsymbol{\epsilon}. \end{aligned}$$

Thus, we have,

$$\begin{aligned} \frac{1}{np}|G(\hat{\boldsymbol{\alpha}}, \hat{\boldsymbol{\beta}}, \hat{W})| &= \frac{1}{np}|\boldsymbol{\epsilon}^\top \hat{W}[V_\alpha(\hat{\boldsymbol{\alpha}} - \boldsymbol{\alpha}) + V_\beta(\hat{\boldsymbol{\beta}} - \boldsymbol{\beta})]| \\ &= \frac{1}{np}|\boldsymbol{\epsilon}^\top \hat{W}[V_\alpha V_\alpha^\top \boldsymbol{\epsilon} + V_\beta(\hat{\boldsymbol{\beta}} - \boldsymbol{\beta})]| \\ &\leq \frac{1}{np}\boldsymbol{\epsilon}^\top \hat{W} V_\alpha V_\alpha^\top \boldsymbol{\epsilon} + \frac{1}{np}|\boldsymbol{\epsilon}^\top \hat{W} V_\beta(\hat{\boldsymbol{\beta}} - \boldsymbol{\beta})| \\ &= \frac{1}{np}\boldsymbol{\epsilon}^\top \hat{W} V_\alpha V_\alpha^\top \boldsymbol{\epsilon} + \frac{1}{np}|\boldsymbol{\epsilon}^\top \hat{W} V_\beta Z^\dagger Z(\hat{\boldsymbol{\beta}} - \boldsymbol{\beta})| \end{aligned}$$

$$\begin{aligned}
&= \frac{1}{np} \boldsymbol{\epsilon}^\top \hat{W} V_\alpha V_\alpha^\top \boldsymbol{\epsilon} + \frac{1}{np} \left| \sum_{i \neq j} \boldsymbol{\epsilon}^\top \hat{W} V_\beta Z_{\mathcal{C}(i,j)}^\dagger Z_{\mathcal{C}(i,j)} (\hat{\boldsymbol{\beta}} - \boldsymbol{\beta}) \right| \\
&\leq \frac{1}{np} \boldsymbol{\epsilon}^\top \hat{W} V_\alpha V_\alpha^\top \boldsymbol{\epsilon} + \frac{1}{np} \sum_{i \neq j} \left| \boldsymbol{\epsilon}^\top \hat{W} V_\beta Z_{\mathcal{C}(i,j)}^\dagger Z_{\mathcal{C}(i,j)} (\hat{\boldsymbol{\beta}} - \boldsymbol{\beta}) \right| \\
&\leq \frac{1}{np} \boldsymbol{\epsilon}^\top \hat{W} V_\alpha V_\alpha^\top \boldsymbol{\epsilon} + \frac{1}{np} \sum_{i \neq j} \|\boldsymbol{\epsilon}^\top \hat{W} V_\beta Z_{\mathcal{C}(i,j)}^\dagger\|_2 \|Z_{\mathcal{C}(i,j)} (\hat{\boldsymbol{\beta}} - \boldsymbol{\beta})\|_2 \\
&\leq \frac{1}{np} \boldsymbol{\epsilon}^\top \hat{W} V_\alpha V_\alpha^\top \boldsymbol{\epsilon} + \frac{1}{np} \max_{i \neq j} \|\boldsymbol{\epsilon}^\top \hat{W} V_\beta Z_{\mathcal{C}(i,j)}^\dagger\|_2 \sum_{i \neq j} \|Z_{\mathcal{C}(i,j)} (\hat{\boldsymbol{\beta}} - \boldsymbol{\beta})\|_2
\end{aligned}$$

Next, we derive high-probability bounds for the terms  $\frac{1}{np} \boldsymbol{\epsilon}^\top \hat{W} V_\alpha V_\alpha^\top \boldsymbol{\epsilon}$  and  $\max_{i \neq j} \|\boldsymbol{\epsilon}^\top \hat{W} V_\beta Z_{\mathcal{C}(i,j)}^\dagger\|_2$ .

**Bounds for  $\frac{1}{np} \boldsymbol{\epsilon}^\top \hat{W} V_\alpha V_\alpha^\top \boldsymbol{\epsilon}$ :**  $\|\hat{W} V_\alpha V_\alpha^\top\|_{sp} \leq \|\hat{W}\|_{sp} \|V_\alpha V_\alpha^\top\|_{sp} \leq (1 + \lambda)$ . Also note that

$$\begin{aligned}
\|\hat{W} V_\alpha V_\alpha^\top\|_F &= \text{tr}(\hat{W} V_\alpha V_\alpha^\top V_\alpha V_\alpha^\top \hat{W}) \\
&= \text{tr}(\hat{W} V_\alpha V_\alpha^\top \hat{W}) \\
&= \text{tr}(\hat{W}^2 V_\alpha V_\alpha^\top) \\
&= \text{tr}(\hat{W}^2 \sum_{i=1}^p \mathbf{v}_i \mathbf{v}_i^\top) \\
&= \sum_{i=1}^p \text{tr}(\hat{W}^2 \mathbf{v}_i \mathbf{v}_i^\top) \\
&= \sum_{i=1}^p \text{tr}(\mathbf{v}_i^\top \hat{W}^2 \mathbf{v}_i) \\
&\leq \sum_{i=1}^p \Lambda_{\max}(\hat{W}^2) \\
&\leq p(1 + \lambda)^2.
\end{aligned}$$

By Lemma 1, we have,

$$\begin{aligned}
P(\boldsymbol{\epsilon}^\top \hat{W} V_\alpha V_\alpha^\top \boldsymbol{\epsilon} \geq t + (1 + \lambda) \sigma^2 p) &\leq P(\boldsymbol{\epsilon}^\top \hat{W} V_\alpha V_\alpha^\top \boldsymbol{\epsilon} \geq t + \sigma^2 \text{tr}(\hat{W} V_\alpha V_\alpha^\top)) \\
&\leq \exp \left\{ - \min \left( \frac{c_1 t^2}{\sigma^4 \|M\|_F}, \frac{c_2 t}{\sigma^2 \|M\|_{sp}} \right) \right\} \\
&\leq \exp \left\{ - \min \left( \frac{c_1 t^2}{\sigma^4 p (1 + \lambda)^2}, \frac{c_2 t}{(1 + \lambda) \sigma^2} \right) \right\}
\end{aligned}$$

Now if we take  $t = \sigma^2 (1 + \lambda) \sqrt{p \log(np)}$ , we have

$$P \left( \frac{1}{np} \boldsymbol{\epsilon}^\top \hat{W} V_\alpha V_\alpha^\top \boldsymbol{\epsilon} \geq \sigma^2 (1 + \lambda) \left[ \frac{1}{n} + \sqrt{\frac{\log(np)}{n^2 p}} \right] \right) \leq \exp \left( - \min \left\{ c_1 \log(np), \frac{c_2}{3} \sqrt{p \log(np)} \right\} \right) \quad (25)$$

**Bounds for  $\max_{i \neq j} \|\boldsymbol{\epsilon}^\top \hat{W} V_\beta Z_{\mathcal{C}(i,j)}^\dagger\|_2$**  Let  $\mathbf{e}_j$  be the  $j$ -th coordinate vector of length  $p \binom{n}{2}$ . Let  $\mathbf{y}_j = \mathbf{e}_j^\top (Z_{\mathcal{C}(i,j)}^\dagger)^\top V_\beta^\top \hat{W} \boldsymbol{\epsilon}$ . Now note that  $\Lambda_{\max}(\hat{W}) \leq (1 + \lambda)$ ,  $\Lambda_{\max}(V_\beta) = 1$  and  $\Lambda_{\max}(Z^\dagger) = \frac{1}{\sqrt{n}}$ . Thus  $\mathbf{y}_j$  is a

one-dimensional sub-Gaussian random variable, with mean 0 and variance at most  $\frac{\sigma^2(1+\lambda)^2}{n}$ . Thus,

$$P(\max_j |y_j| \geq z) \leq p \binom{n}{2} P(|y_j| \geq z) \leq 2p \binom{n}{2} \exp \left\{ -\frac{nz^2}{2\sigma^2(1+\lambda)^2} \right\} \quad (26)$$

Now, if we choose  $z = 2\sigma(1+\lambda)\sqrt{\frac{\log(p\binom{n}{2})}{n}}$ , we get

$$P\left(\max_{i \neq j} \|\epsilon^\top \hat{W} V_\beta Z_C^\dagger\|_\infty \geq 2\sigma(1+\lambda)\sqrt{\frac{\log(p\binom{n}{2})}{n}}\right) = P\left(\max_j |y_j| \geq 2\sigma(1+\lambda)\sqrt{\frac{\log(p\binom{n}{2})}{n}}\right) \leq \frac{2}{p\binom{n}{2}} \quad (27)$$

Now since there are only  $p$  indices in  $\mathcal{C}(i, j)$ , we have

$$\|\epsilon^\top \hat{W} V_\beta Z_C^\dagger(i, j)\|_2 \leq \sqrt{p} \|\epsilon^\top \hat{W} V_\beta Z_C^\dagger(i, j)\|_\infty.$$

Observe that

$$\frac{1}{np} \max_{i \neq j} \|\epsilon^\top \hat{W} V_\beta Z_C^\dagger(i, j)\|_2 \leq \frac{1}{\sqrt{n^2 p}} \max_{i \neq j} \|\epsilon^\top \hat{W} V_\beta Z_C^\dagger(i, j)\|_\infty = \frac{1}{\sqrt{n^2 p}} \|\epsilon^\top \hat{W} V_\beta Z^\dagger\|_\infty.$$

Thus,

$$\begin{aligned} & P\left(\frac{1}{np} \max_{i \neq j} \|\epsilon^\top \hat{W} V_\beta Z_C^\dagger(i, j)\|_2 \geq 2\sigma(1+\lambda)\sqrt{\frac{\log(p\binom{n}{2})}{n^3 p}}\right) \\ & \leq P\left(\max_{i \neq j} \|\epsilon^\top \hat{W} V_\beta Z^\dagger\|_\infty \geq 2\sigma(1+\lambda)\sqrt{\frac{\log(p\binom{n}{2})}{n}}\right) \\ & \leq \frac{2}{p\binom{n}{2}}. \end{aligned}$$

We see that when  $\gamma' > 2\sigma(1+\lambda)\sqrt{\frac{\log(p\binom{n}{2})}{np}}$ , we have

$$P\left(\frac{\gamma'}{n} < \frac{1}{np} \max_{i \neq j} \|\epsilon^\top \hat{W} V_\beta Z_C^\dagger(i, j)\|_2\right) \leq \frac{2}{p\binom{n}{2}} \quad (28)$$

Combining equations (25) and (28) implies that

$$\frac{1}{np} |G(\hat{\alpha}, \hat{\beta}, (\hat{W}))| \leq \sigma^2(1+\lambda) \left[ \frac{1}{n} + \sqrt{\frac{\log(np)}{n^2 p}} \right] + \frac{\gamma'}{n} \sum_{i \neq j} \|Z_{\mathcal{C}(i, j)}(\hat{\beta} - \beta)\|_2 \quad (29)$$

holds with probability at least  $1 - \frac{2}{p\binom{n}{2}} - \exp\left(-\min\left\{c_1 \log(np), \frac{c_2}{3} \sqrt{p \log(np)}\right\}\right)$ . Thus, from equation (24) and (29), we arrive at the inequality

$$\begin{aligned} & \frac{1}{2np} \|V_\alpha(\hat{\alpha} - \alpha) + V_\beta(\hat{\beta} - \beta)\|_{\hat{W}}^2 + \gamma' \sum_{i \neq j} \|Z_{\mathcal{C}(i, j)} \hat{\beta}\|_2^2 \\ & \leq \sigma^2(1+\lambda) \left[ \frac{1}{n} + \sqrt{\frac{\log(np)}{n^2 p}} \right] + \frac{\gamma'}{n} \sum_{i \neq j} \|Z_{\mathcal{C}(i, j)}(\hat{\beta} - \beta)\|_2 + \gamma' \sum_{i \neq j} \|Z_{\mathcal{C}(i, j)} \beta\|_2^2 \end{aligned}$$

Finally upon rearranging, we obtain

$$\begin{aligned}
& \frac{1}{2np} \|V_{\alpha}(\hat{\alpha} - \alpha) + V_{\beta}(\hat{\beta} - \beta)\|_{\hat{W}}^2 \\
& \leq \sigma^2(1 + \lambda) \left[ \frac{1}{n} + \sqrt{\frac{\log(np)}{n^2 p}} \right] + \gamma' \sum_{i \neq j} \left[ \frac{\|Z_{C(i,j)} \hat{\beta}\|_2}{n} - \|Z_{C(i,j)} \hat{\beta}\|_2^2 \right] + \frac{\gamma'}{n} \sum_{i \neq j} \|Z_{C(i,j)} \beta\|_2 \\
& + \gamma' \sum_{i \neq j} \|Z_{C(i,j)} \beta\|_2^2 \\
& \leq \sigma^2(1 + \lambda) \left[ \frac{1}{n} + \sqrt{\frac{\log(np)}{n^2 p}} \right] + \gamma' n(n-1) \frac{1}{n^2} + \frac{\gamma'}{n} \sum_{i \neq j} \|Z_{C(i,j)} \beta\|_2 + \gamma' \sum_{i \neq j} \|Z_{C(i,j)} \beta\|_2^2 \\
& \leq \sigma^2(1 + \lambda) \left[ \frac{1}{n} + \sqrt{\frac{\log(np)}{n^2 p}} \right] + \gamma' \left(1 - \frac{1}{n}\right) + \frac{\gamma'}{n} \sum_{i \neq j} \|D_{C(i,j)} \mathbf{u}\|_2 + \gamma' \sum_{i \neq j} \|D_{C(i,j)} \mathbf{u}\|^2
\end{aligned}$$

□

## C Additional figures and tables

### C.1 Dendrograms, simulation study 4.2

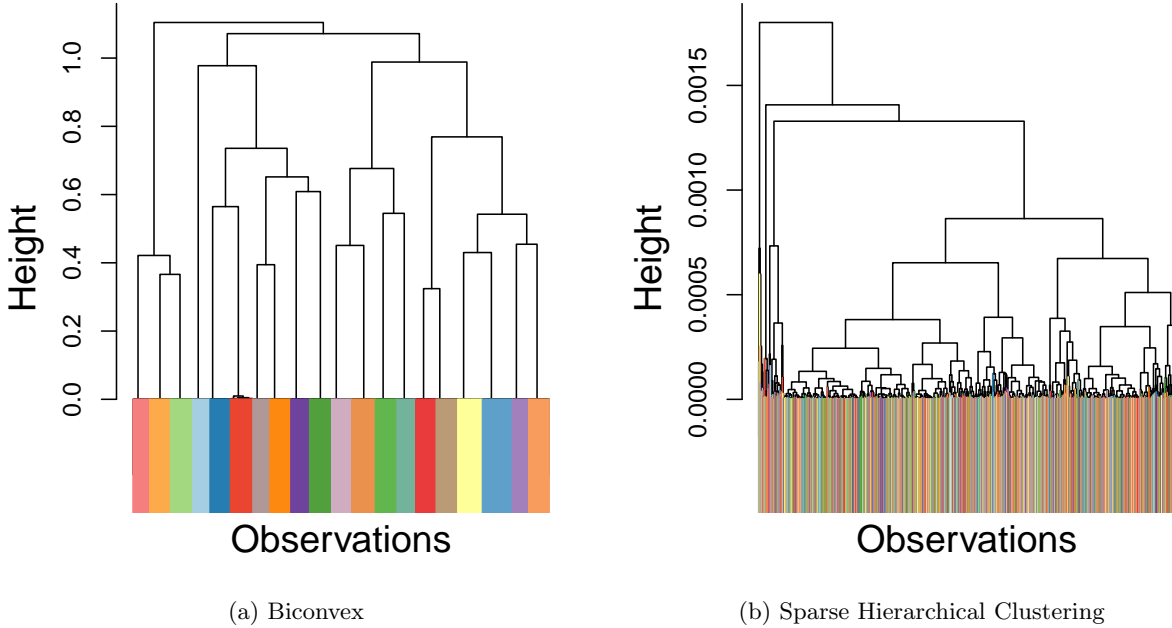


Figure 9: Dendrograms, color coded with the ground truth, produced by biconvex clustering and sparse hierarchical clustering algorithms on the simulated data in Section 4.2. Biconvex clustering perfectly recovers the ground truth using a dynamic tree cut, and it is clear that this can be achieved for a generous range of heights. In contrast sparse hierarchical clustering failed to recover the true clusters, and the dendrogram structure in panel (b) provides insight on why this is the case.

## C.2 Sensitivity to Random Restarts

In this section, we will study the effects of random initialization of the feature weights. We generated three datasets each with the first five features revealing the cluster structure of the dataset. We then append  $d$  many features to the dataset, each generated from a standard normal distribution. The datasets are generated using the procedures described in Section 4.1. For each of the datasets, we start with a randomly chosen initialization of feature weights and iterate until convergence. We initialize each of the feature weights from  $Unif(0, 1)$ , and repeat the experiment over 100 trials. Boxplots of the resulting feature weight estimates are shown in Figure 10. It can be easily observed from Figure 10 that the algorithm can consistently identifies the relevant variables, while giving no weight to the unimportant ones. It also consistently recovers the cluster structure in each of the experiments, demonstrating stability to initial guess of  $w$ .

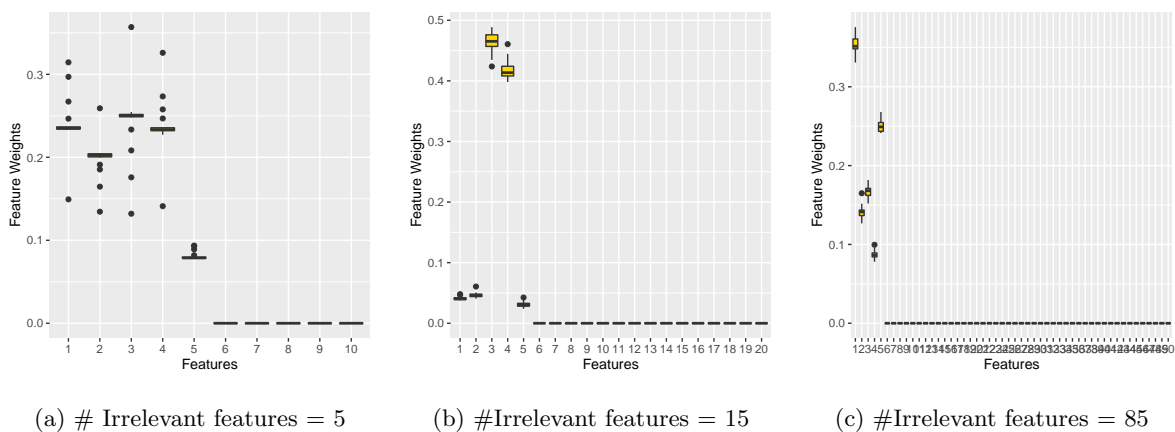


Figure 10: Box plot of top ranked features selected by BCC algorithm under random initialization of  $w$  as the number of irrelevant features (d) varies (detailed in Section C.2). We see the performance of the algorithm appears to be fairly stable even in high dimensions.

## C.3 Case Study on Leukemia Data

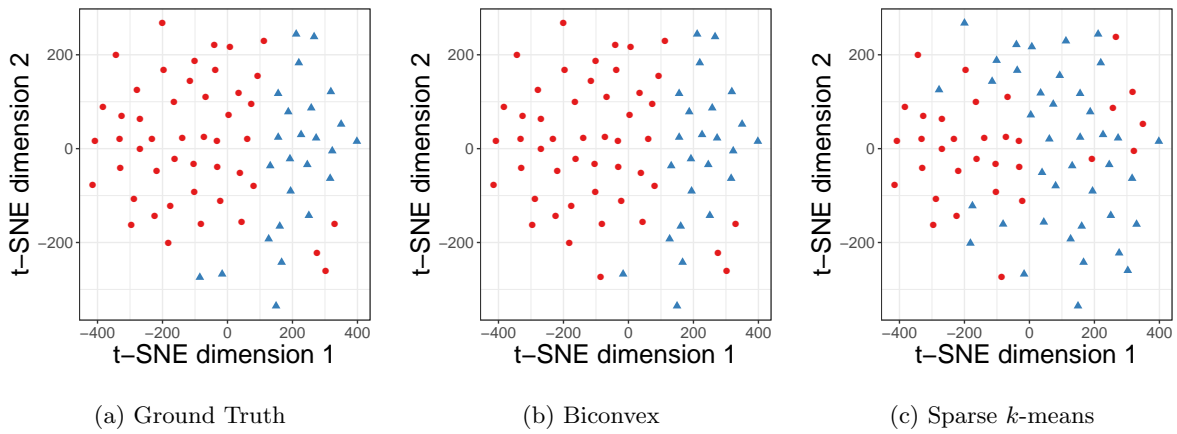


Figure 11: Comparison of solutions in t-SNE embedding, leukemia dataset. We see that the solution obtained under our method closely resembles the ground truth.